Supporting Information

Benzimidazolin-2-iminato Hafnium Complexes: Synthesis, Characterization, and Catalytic Addition of Alcohols to Carbodiimides.

Maxim Khononov,[1] Heng Liu, [1] Natalia Fridman,[1] Matthias Tamm,[2] and Moris S. Eisen.[1*]

[1] Schulich Faculty of Chemistry, Technion-Israel Institute of Technology, Technion City 32000 Israel

[2]Institut für Anorganische und Analytische Chemie, Technische Universität Braunschweig, Hagenring 30, 38106 Braunschweig, Germany.

Contents

1. General considerations

All manipulations of air-sensitive materials were performed with the rigorous exclusion of oxygen and moisture in flamed Schlenk-type glassware on a high vacuum line (10^{-5} Torr) or in nitrogen-filled MBraun and Vacuum Atmospheres gloveboxes with a medium capacity recirculator (1−2 ppm oxygen). Argon and nitrogen were purified by passage through a MnO oxygen removal column and a Davison 4 Å molecular sieve column. Analytically pure solvents were dried and stored with Na/K alloy and degassed by three

freeze−pump−thaw cycles before use (hexane, toluene, benzene-d6, toluene-d8). BenzIm^{Dipp}NH, benzIm^{Mes}NH, Im^{Mes}NH, and the metal precursor, hafnium tetrabenzyl were synthesized according to published literature procedures.[1–3] 1,3-diisopropylcarbodiimide (Sigma Aldrich) was dried by vacuum transfer. MeOH, EtOH, ^{i}PrOH, ^{t}BuOH, were distilled under CaH_2 and stored over 4Å molecular sieves. PhOH, 2,6-Me_2PhOH, 2,4-tBu_2PhOH, and 1,3-di-p-tolylcarbodiimide (Sigma Aldrich) were dried for 12 hours on a high vacuum line (10^{-5} torr) and stored in a glovebox prior to use. Deuterated MeOH and ^{t}BuOH (Sigma Aldrich) were prepared using a similar method according to published procedures. NMR spectra were recorded on Avance 200, Avance 300, Avance 400, Avance 500, and Avance 600 Bruker spectrometers. Chemical shifts for ^{1}H NMR, ^{13}C NMR measurements are reported in ppm and referenced using residual proton or carbon signals of the deuterated solvent relative to tetramethylsilane. For all the complexes, the formation of the corresponding carbides precludes the elemental analysis (with or without V_2O_5). HRMS experiments were performed at 200 °C (source temperature) on a Maxis Impact (Bruker) mass spectrometer using the APCI solid probe methodology. For X-ray crystallographic measurements, the single- crystalline material was immersed in perfluoropolyalkylether oil and was quickly fished with a glass rod and mounted on a Kappa CCD diffractometer under a cold stream of nitrogen. Data collection was performed using monochromated Mo Kα radiation using φ and ω scans to cover the Ewald sphere. Accurate cell parameters were obtained with the amount of indicated reflections. The structure was solved by SHELXS-97 direct methods and refined by the SHELXL-97 program package.[4–6]

2. General procedure for the synthesis of hafnium(IV) complexes **1-3**

Synthesis of mono(benzimidazolin-2-iminato) hafnium(IV) complexes **1** and **2**: A toluene solution of the respective benz(imidazolin-2-imine) Im^{R}NH (56.5 mg, 0.184mmol) in 5 mL of toluene was added dropwise to a pre-prepared solution of hafnium tetrabenzyl (100 mg 0.184 mmol) in toluene (5 mL) at room temperature. The reaction mixture was stirred overnight at room temperature. The solvent was removed under vacuum to afford the crude complexes **1−2**. In each case, the product was recrystallized from a concentrated toluene solution at −35°C to yield compounds **1** and **2** as crystalline materials.

1-(2,6-diisopropylphenyl)-3-methylbenzimidazolin-2-imine hafnium tribenzyl [(BenzImDippN)HfBn$_3$], (Complex **1**): Yield: 0.128 g, 0.168mmol, 92%

1-(2,4,6-trimethylphenyl)-3-methylbenzimidazolin-2-imine hafnium tribenzyl [(BenzImMesN)HfBn$_3$], (Complex **2**): Yield: 0.114 g, 0.160 mmol, 87%

Synthesis of mono 1-(2,4,6-trimethylphenyl)-3-methylimidazolin-2-imine-hafnium tribenzyl [(ImMesN)HfBn$_3$], (Complex **3**): A toluene solution of the respective (imidazolin-2-imine) ImMesNH (19.79 mg, 0.092mmol) in 5 mL of toluene was added

dropwise to a preprepared solution of hafnium tetrabenzyl (50 mg 0.092 mmol) in toluene (5 mL) at room temperature. The solvent was removed under vacuum to afford crude compound 3. Complex **3** was recrystallized from a concentrated toluene solution at −35°C to yield 0.049 g, 0.0736 mmol 80% yield of the crystalline materials.

2.1 ^{1}H NMR and ^{13}C NMR of complexes

2.1.1 ^{1}H NMR and ^{13}C NMR of complex **1**:

^{1}H NMR (600 MHz, C_6D_6) δ 7.27 (t, 1H, H-Ar), 7.18 (m, 9H, H-Ph), 7.15(m, 3H, H-Ph), 6.97(m, 6H, H-Ph), 6.85(s, 1H, H-Ar), 6.75(s, 1H, H-Ar), 6.60(d, 1H, H-Ar), 6.38(d, 1H, H-Ar), 2.97(s, 3H, C*H*$_3$), 2.72(m, 2H, C*H*(CH$_3$)$_2$), 1.61(s, 6H, C*H*$_2$Ph), 1.24(d, 6H, CH(C*H*$_3$)$_2$), 0.92(d, 6H, CH(C*H*$_3$)$_2$). ^{13}C NMR (150 MHz, C_6D_6) δ 148.19, 145.53, 142.75, 131.05, 130.35, 129.44, 128.81, 124.20, 122.36, 108.70, 108.08, 72.30, 28.68, 27.56, 24.17, 23.67. MS (APCI) for $C_{41}H_{45}HfN_3$ = 759.7492.

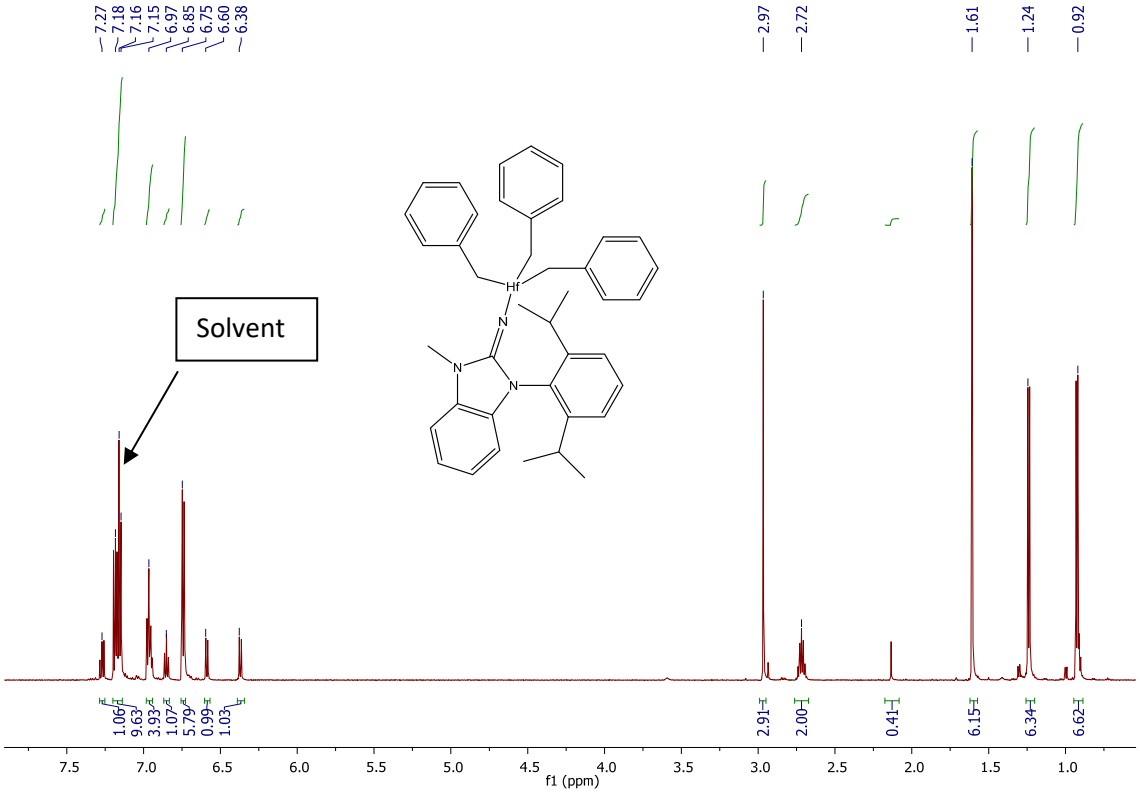

Figure S1. ^{1}H NMR of complex **1**.

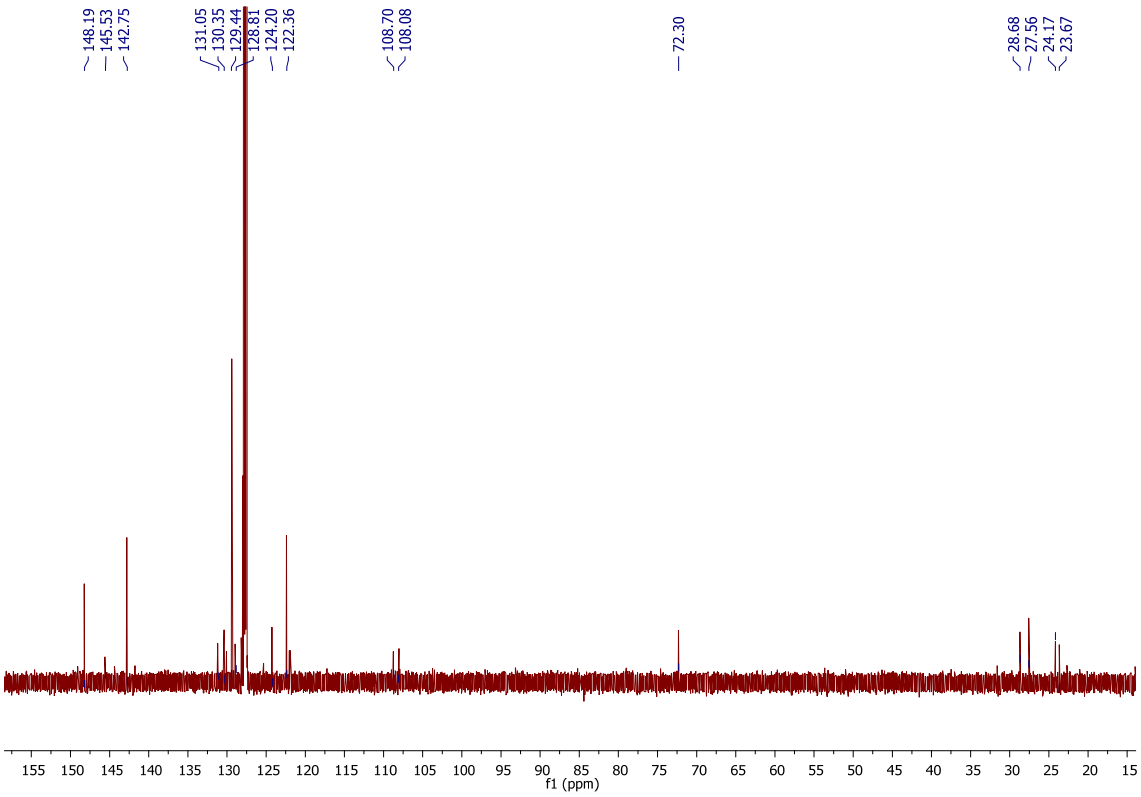

Figure S2. ^{13}C NMR of complex **1**.

2.1.2 ^{1}H NMR and ^{13}C NMR of complex **2**:

^{1}H NMR (500 MHz, C_6D_6) δ 7.31 (d, 1H, H-Ar), 7.13 - 6.99(m, 15H, H-Ar) 6.79 (d, 1H, H-Ar), 6.63 (d, 1H, H-Ar), 6.36(d, 1H, H-Ar), 2.88 (s, 3H, C*H*$_3$), 2.10 (s, 9H, C*H*$_3$-Ar), 2.00 (s, 6H, C*H*$_2$-Ph). ^{13}C NMR (126 MHz, C_6D_6) δ 146.13, 142.49, 139.05, 137.47, 130.39, 129.19, 125.37, 122.26, 107.87, 71.18, 27.39, 20.65, 17.34. MS (APCI) for : $C_{38}H_{39}HfN_3$+H (M+H) -C_6H_5 = 642.3962

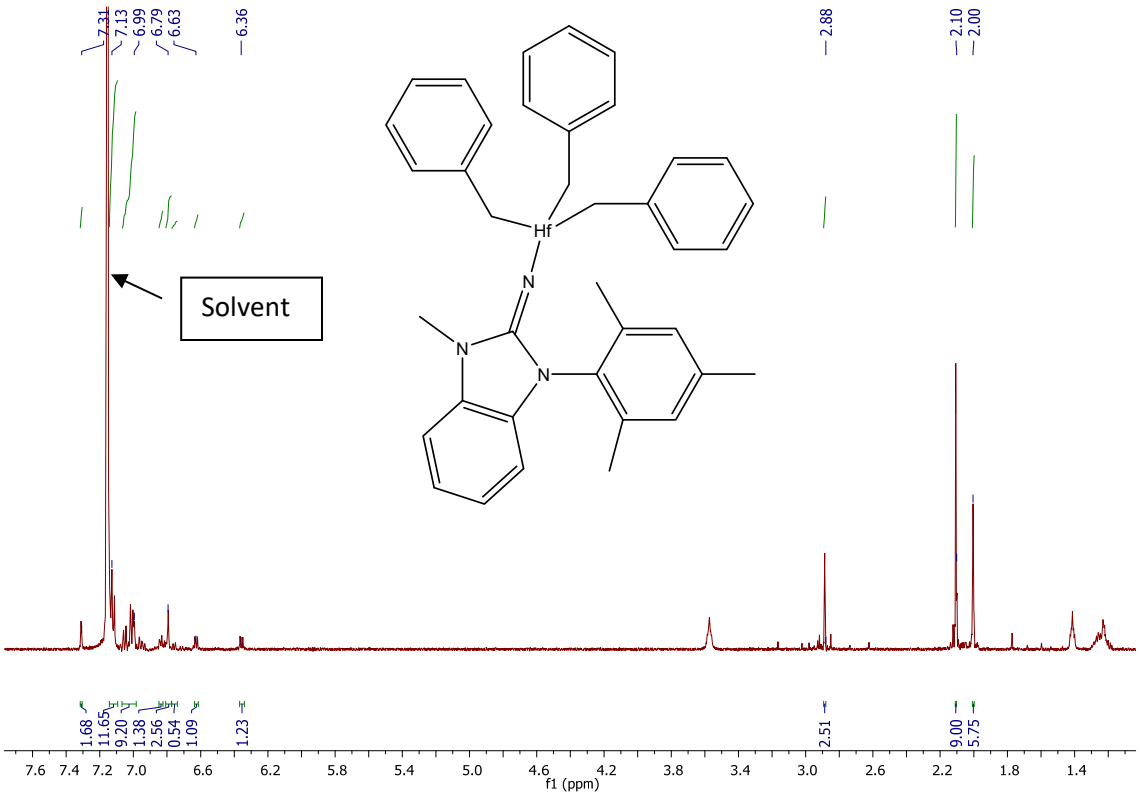

Figure S3. ^{1}H NMR of complex **2**.

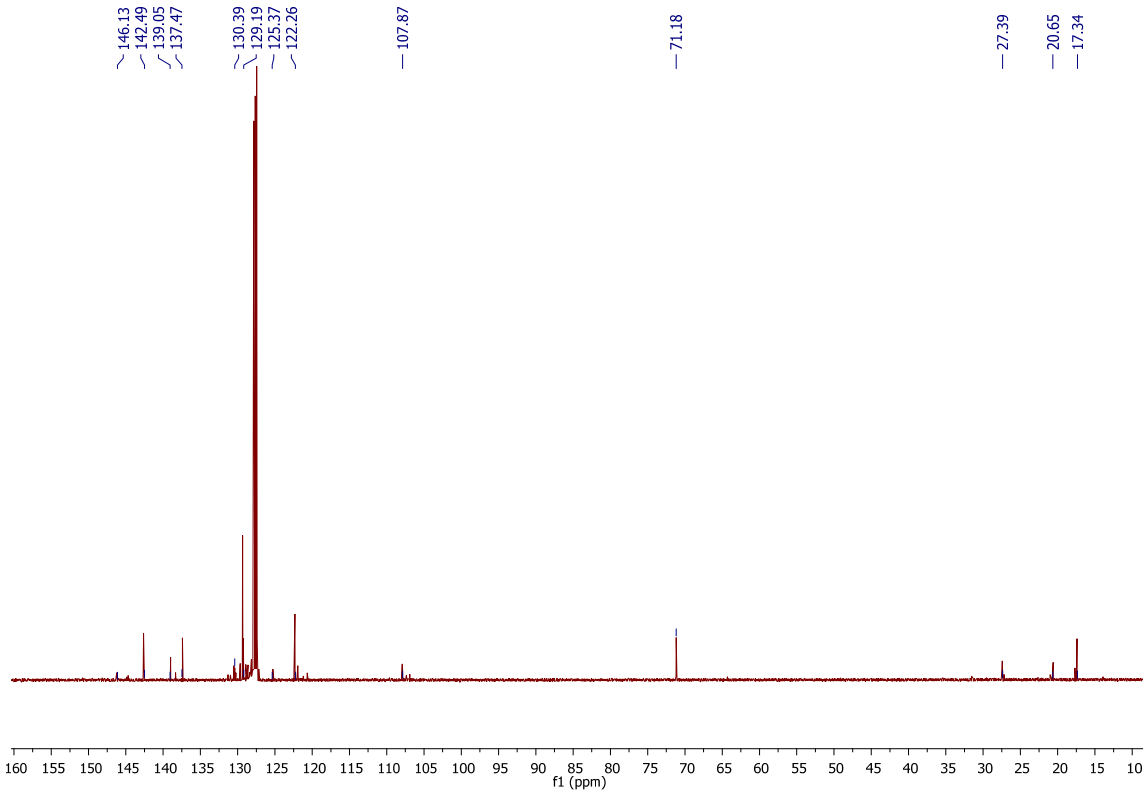

Figure S4. ^{13}C NMR of complex **2**.

2.1.3 ^{1}H NMR and ^{13}C NMR of complex **3**:

^{1}H NMR (300 MHz, C_7D_8) δ 7.07 (m, 7H, *H*-Ph), 6.89 (t, 3H, H-Ar), 6.75 (s, 3H, H-Ar), 6.54 (d, 6H, H-Ph), 5.58 (s, 1H, C*H*), 5.51 (s, 1H, C*H*), 2.74 (s, 3H, CH_3), 2.10 (s, 3H, CH_3-Ar), 2.01 (s, 6H, CH_3-Ar), 1.48(s, 6H, CH_2-Ph).

^{13}C NMR (75 MHz, C_7D_8) δ 145.06, 143.38, 138.43, 136.96, 136.50, 133.17, 128.98, 128.67, 128.36, 128.04, 127.77, 127.45, 127.20, 127.13, 121.67, 112.26, 110.57, 69.60, 31.52, 30.93, 17.48. MS (APCI) for $C_{34}H_{37}HfN_3$+N (from the APCI) (M+N) = 680.4198.

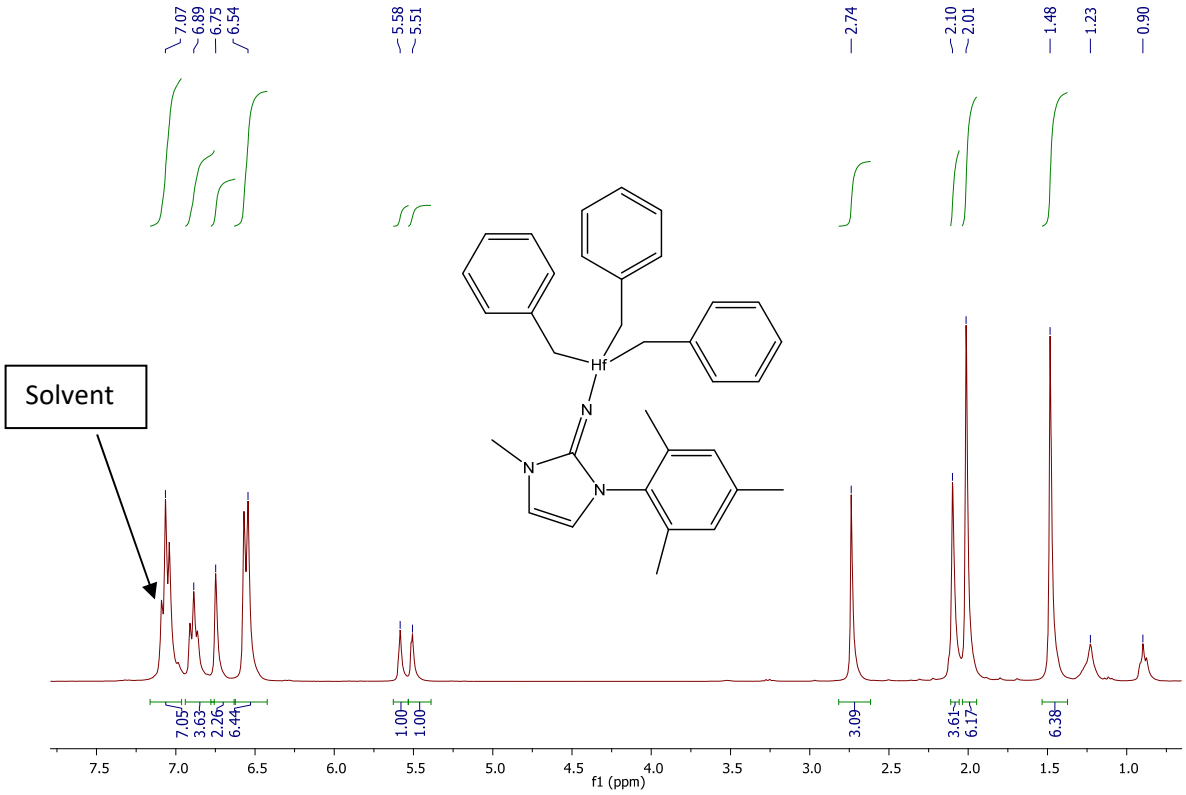

Figure S5. ^{1}H NMR of complex **3**.

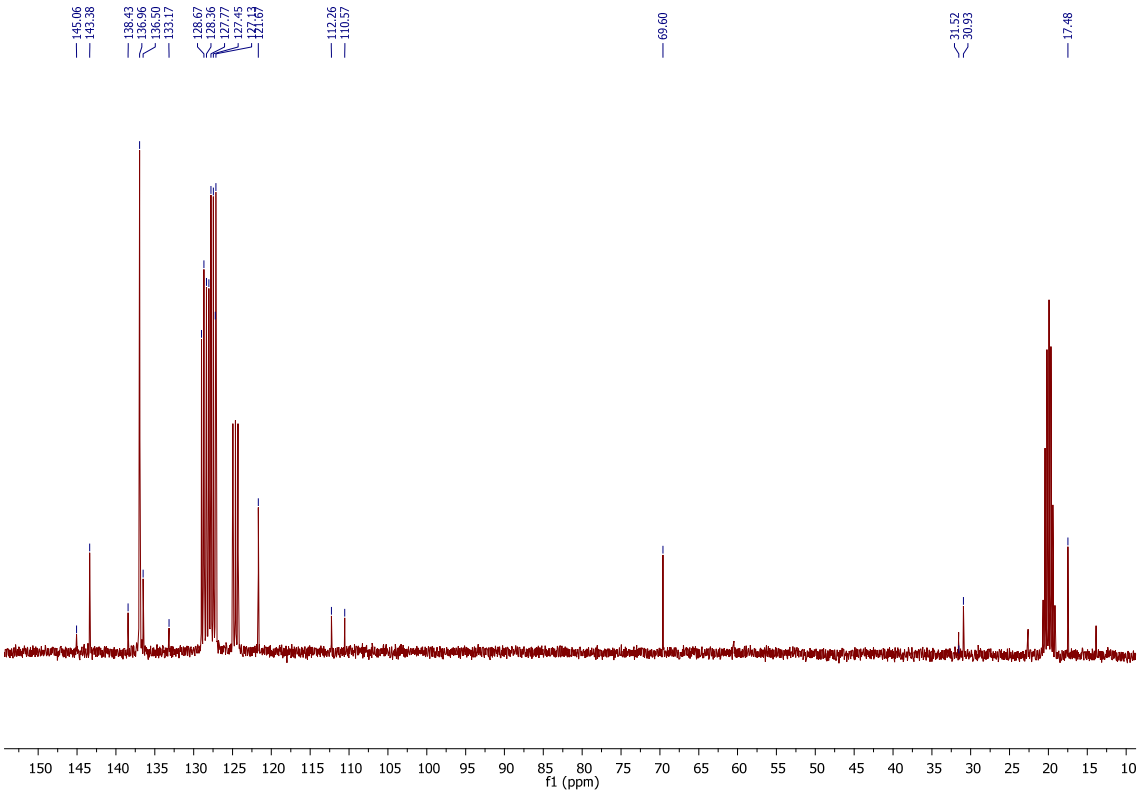

Figure S6. ^{13}C NMR of complex **3**.

2.1.4 ^{1}H NMR and ^{13}C NMR of complex **4**:

^{1}H NMR (300 MHz, C_6D_6) δ 7.10 (m, 3H, *H*-Ph) , 6.82(t, 1H, H-Ar), 6.70(t, 1H, H-Ar), 6.50(d, 1H, H-Ar), 6.17(d, 1H, H-Ar), 5.22 (s,1H,N*H*), 3.62(s, 3H, CH_3), 2.66(m, 2H, CH(CH_3)$_2$), 1.36 (s, 36H, CH_3), 1.17 (d, 6H, CH(CH_3)$_2$), 0.84 (d, 6H, CH(CH_3)$_2$) ^{13}C NMR (125 MHz, C_6D_6) δ 149.09, 132.31, 130.31, 128.95, 125.17, 124.86, 120.77, 107.02, 33.29, 28.12, 23.92. MS (APCI): $C_{36}H_{61}HfN_3O_4$ (M) = 778.6758.

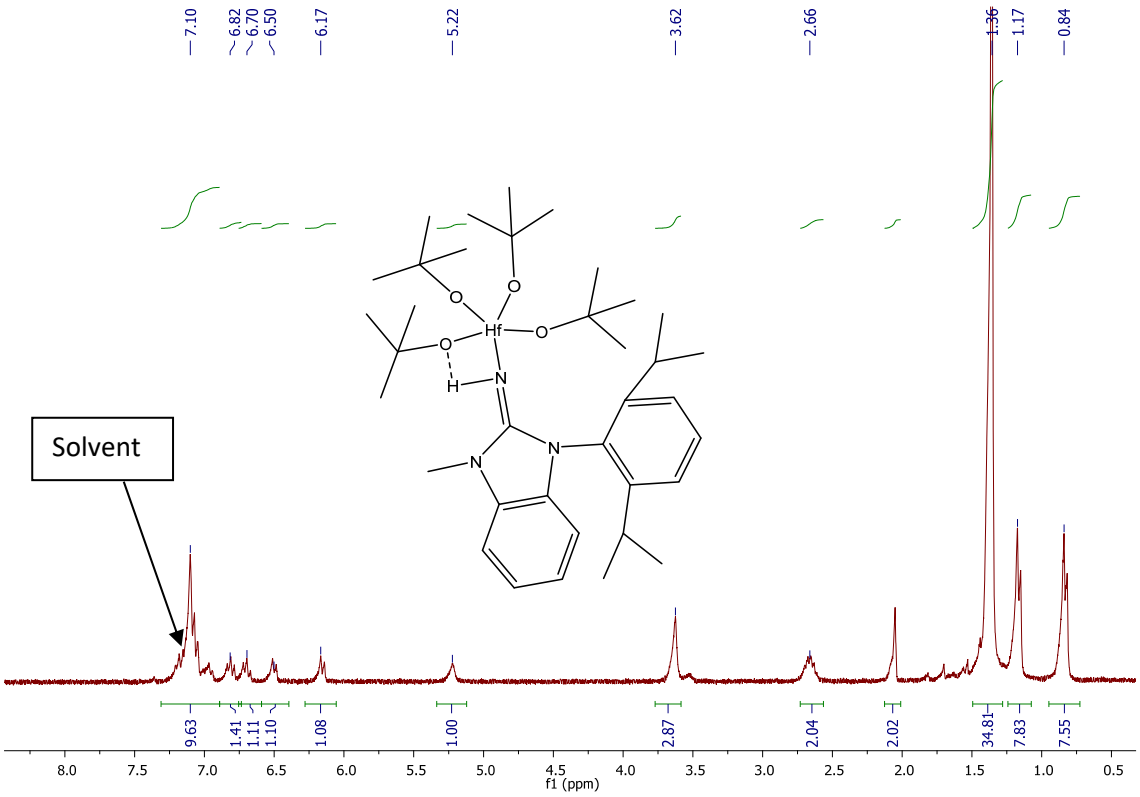

Figure S7. ^{1}H NMR of complex **4**.

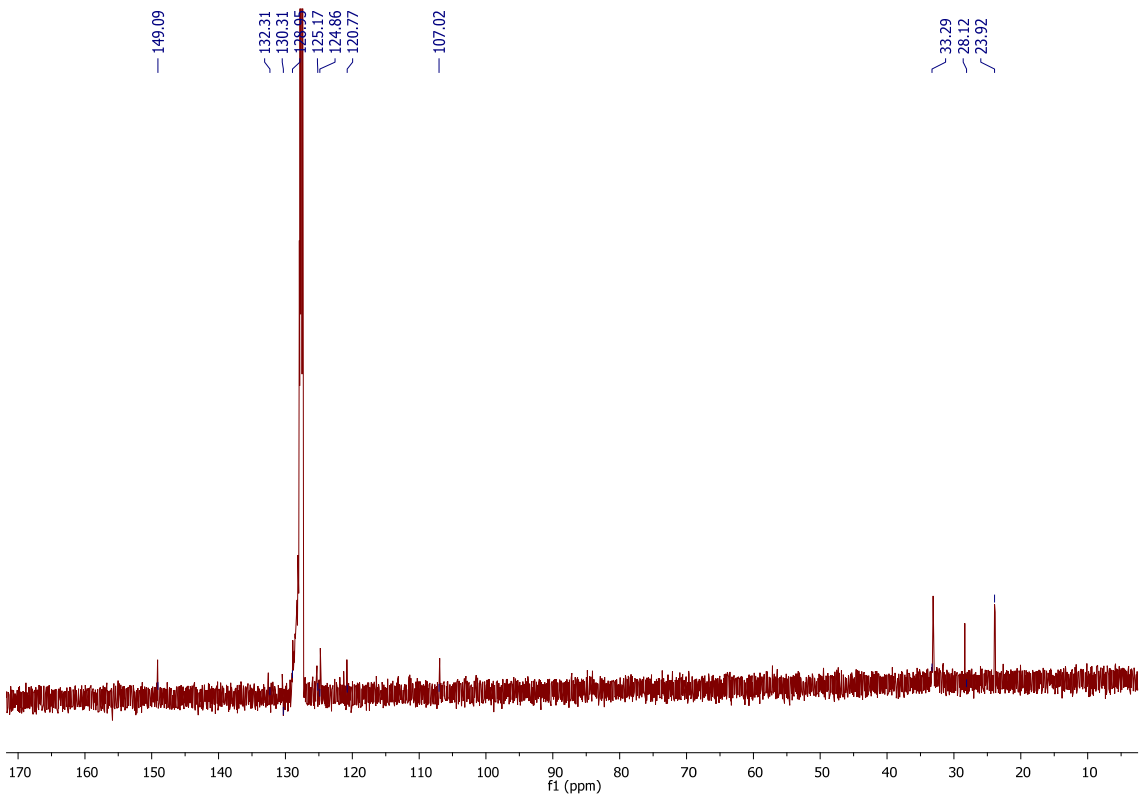

Figure S8. ^{13}C NMR of complex **4**.

2.1.5 ^{1}H NMR and ^{13}C NMR of complex **5**:

^{1}H NMR (200 MHz, C_6D_6) δ 7.25- 7.09 (m, 5H, Ar), 2.21 (s, 3H, C*H*$_3$-Ph), 1.42 (s, 9H, C(C*H*$_3$)$_3$). ^{13}C NMR (50 MHz, C_6D_6) δ 129.06, 125.41, 91.40, 32.67, 21.25.

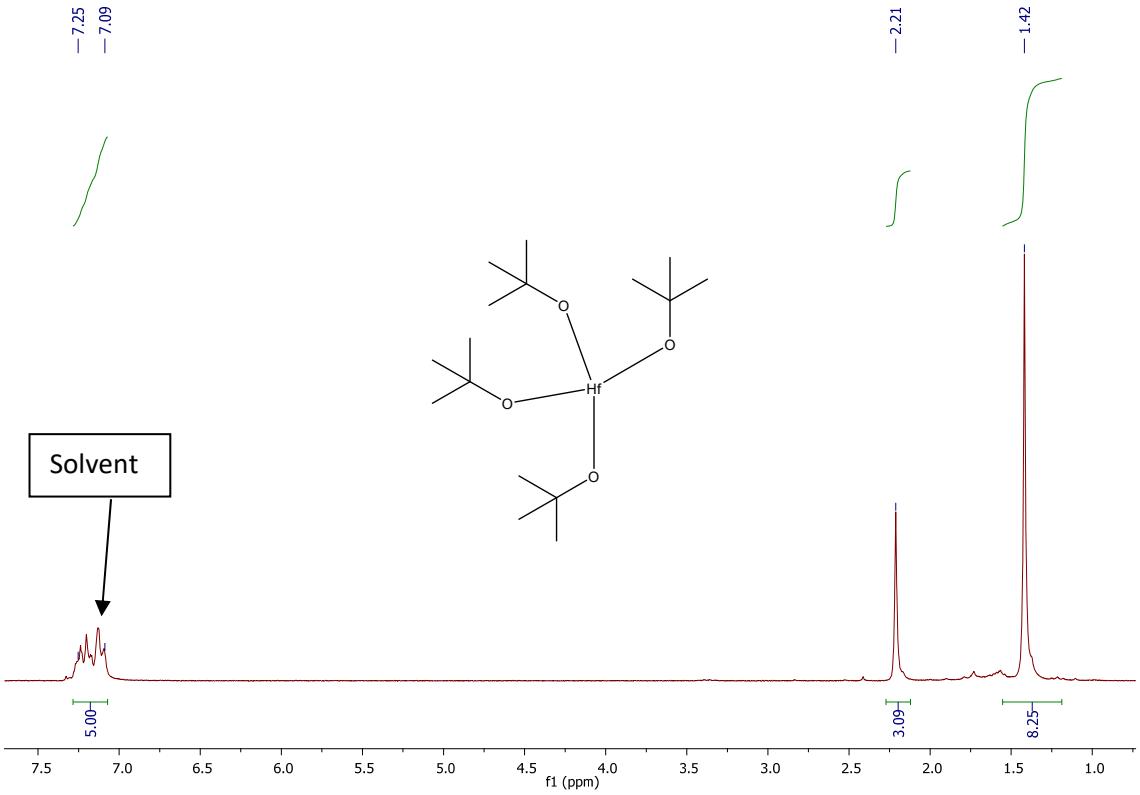

Figure S9. ^{1}H NMR of complex **5**.

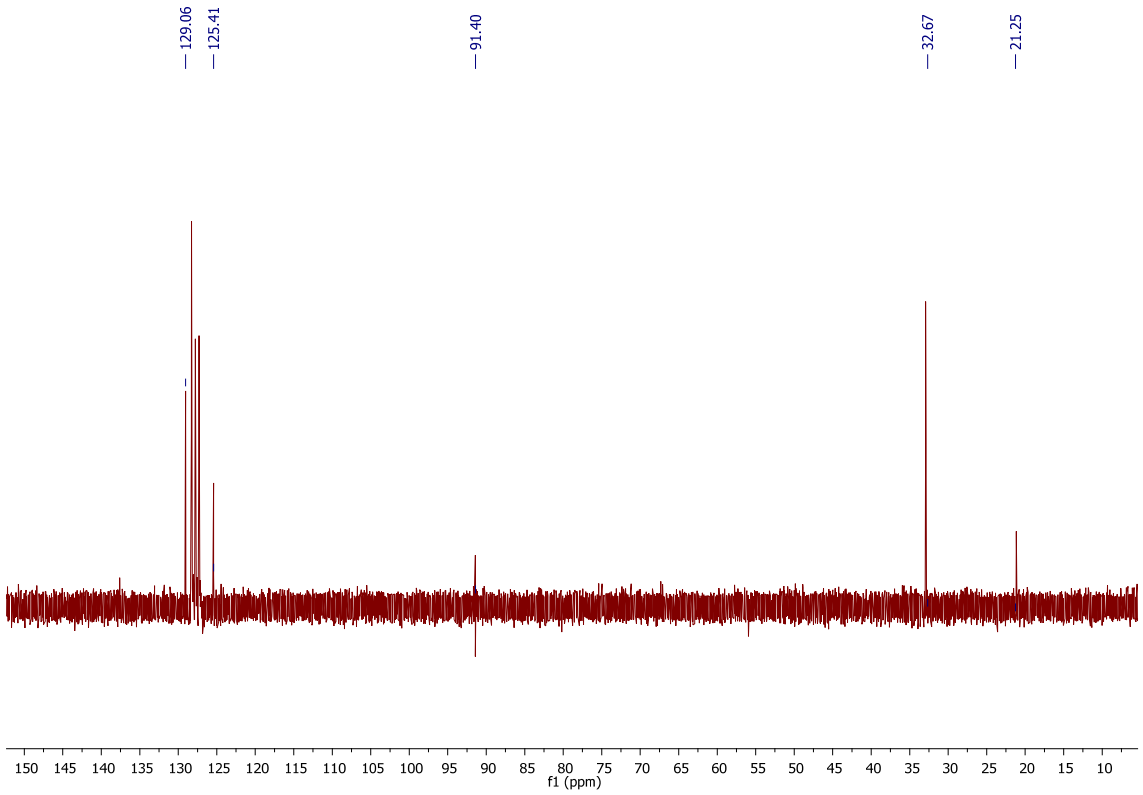

Figure S10. ^{13}C NMR of complex **5**.

2.1.6 ^{1}H NMR and ^{13}C NMR of complex **6**:

^{1}H NMR (500 MHz, C_6D_6) δ 7.19, 6.97(m, 20H, *H*-Ph), 6.75-6.57 (m, 5H, *H*-Ar), 6.12 (d, 1H, *H*-Ar), 6.03 (d, 1H, *H*-Ar), 3.03 (s, 3H, C*H*$_3$), 2.03 (m, 2H, C*H*(CH$_3$)$_2$), 1.02 (d, 6H, C*H*$_3$), 0.68 (d, 6H, C*H*$_3$). ^{13}C NMR (125 MHz, C_6D_6) δ 156.22, 147.72, 132.00, 128.96, 125.38, 119.92, 115.21, 31.38, 28.64, 23.70, 23.41, 22.57, 13.76. MS(APCI) for $C_{50}H_{51}HfN_3O_5$+H+N (from the APCI) (M+H+N) -C_6H_5 = 890.8096.

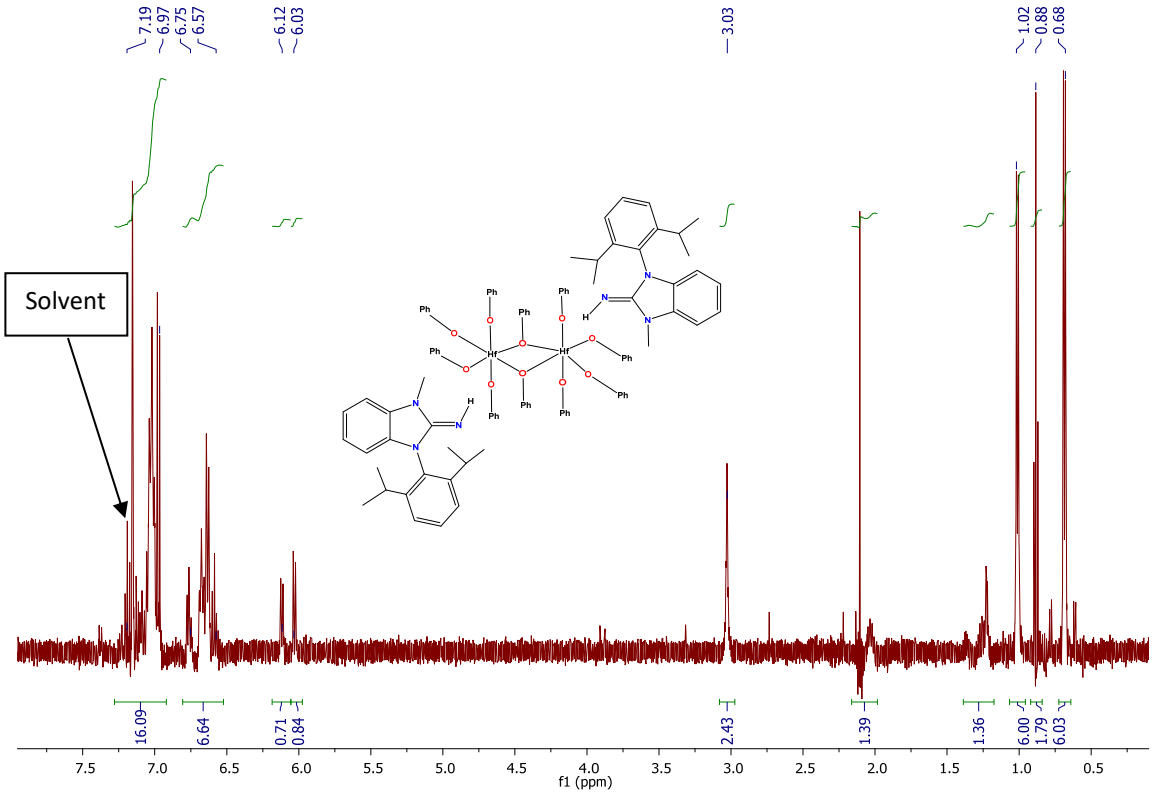

Figure S11. ^{1}H NMR of complex **6**.

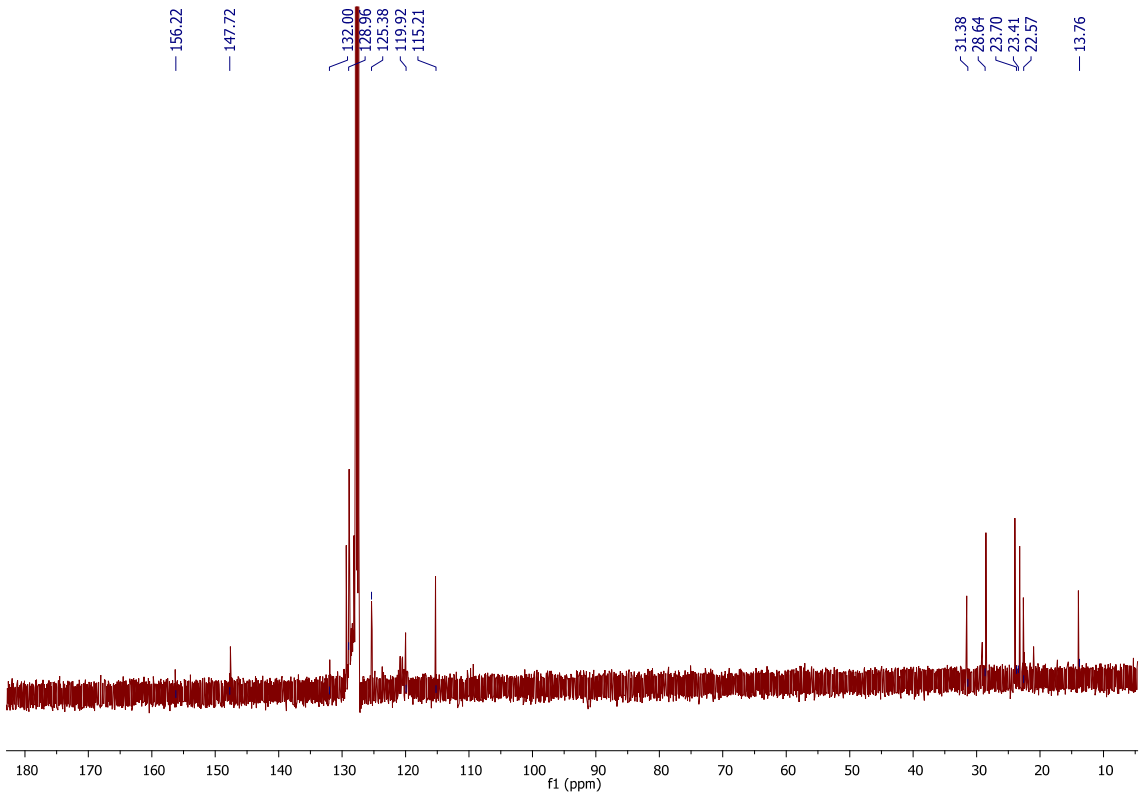

Figure S12. ^{13}C NMR of complex **6**.

2.1.7 ^{1}H NMR and ^{13}C NMR of complex **7:**

^{1}H NMR (300 MHz, C_6D_6) δ 6.96 (d, 10H, H_{Ar}), 6.90-6.86 (t, 5H, H_{Ar}), 6.76-6.65(m, 5H, H_{Ar}), 6.17(dd, 2H, H_{Ar}), 5.68(S, 1H, N*H*), 4.02(S, 1H, O*H*), 3.35(S, 3H, CH_3), 2.39(S, 3H, CH_3), 2.32(m, 2H, CH(CH_3)$_2$), 1.96(S, 6H, CH_3), 0.95 (d, 6H, CH_3), 0.76 (d, 6H, CH_3). ^{13}C NMR (75 MHz, C_6D_6) δ 159.65, 155.83, 148.21, 131.49, 131.27, 130.92, 128.42, 128.20, 126.29, 125.21, 125.10, 119.98, 119.21, 115.22, 108.76, 107.05, 28.97, 28.36, 24.40, 22.83, 17.41, 15.41. MS (APCI) for $C_{60}H_{70}HfN_3O_5$ (low intensity signal): 1093.9998.

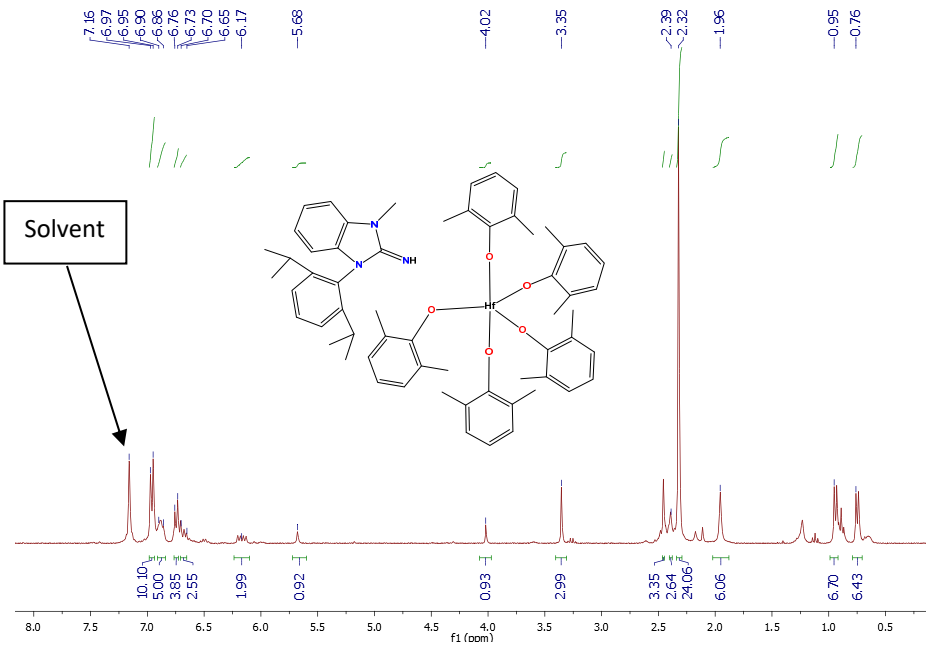

Figure S13. ^{1}H NMR of complex **7**.

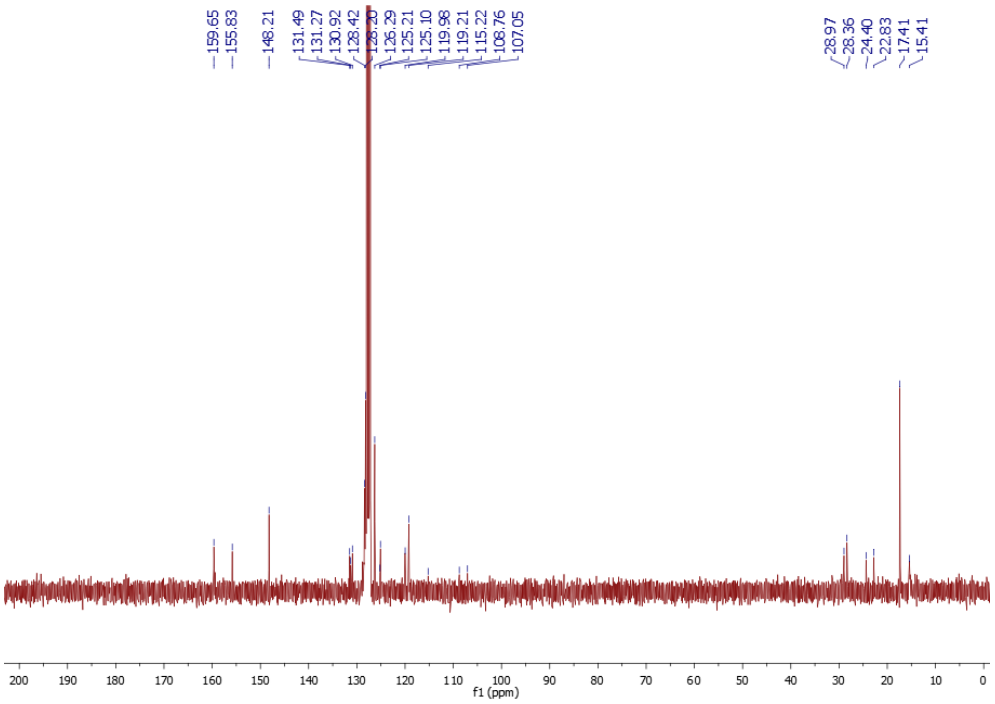

Figure S14. ^{13}C NMR of complex **7**.

3. General procedure for the catalytic addition of alcohols into carbodiimides.

For Hf(IV) complexes, in a sealable J. Young NMR tube was loaded with 5.8μmol of the desired catalyst from a stock solution in C_6D_6 inside the glove box, followed by the addition of a prepared solution of alcohols (50 equiv.) and carbodiimide (50 equiv.), the total volume of the solution was 600 μL and the solvent was C_6D_6. Samples were taken out of the glove box and the reaction progress was monitored by ^{1}H NMR spectroscopy. The crude mixtures were analyzed using ^{1}H NMR, the values were compared to previous literature. [2,7]

3.1. Insertion of MeOH into di-p-tolylcarbodiimide with complexes **1-3**

The insertion of methanol (11.8 μL, 0.29 mmol) into di-p-tolylcarbodiimide (64.98.4mg, 0.29 mmol) was carried out according to the general procedure described above.

^{1}H NMR (300 MHz, C_6D_6) δ 6.96 – 6.69 (m, 8H, *H*Ar), 5.81 (s, 1H, NH), 3.68 (s, 3H, CH_3), 2.11 (s, 3H, CH_3), 2.00 (s, 3H, CH_3).

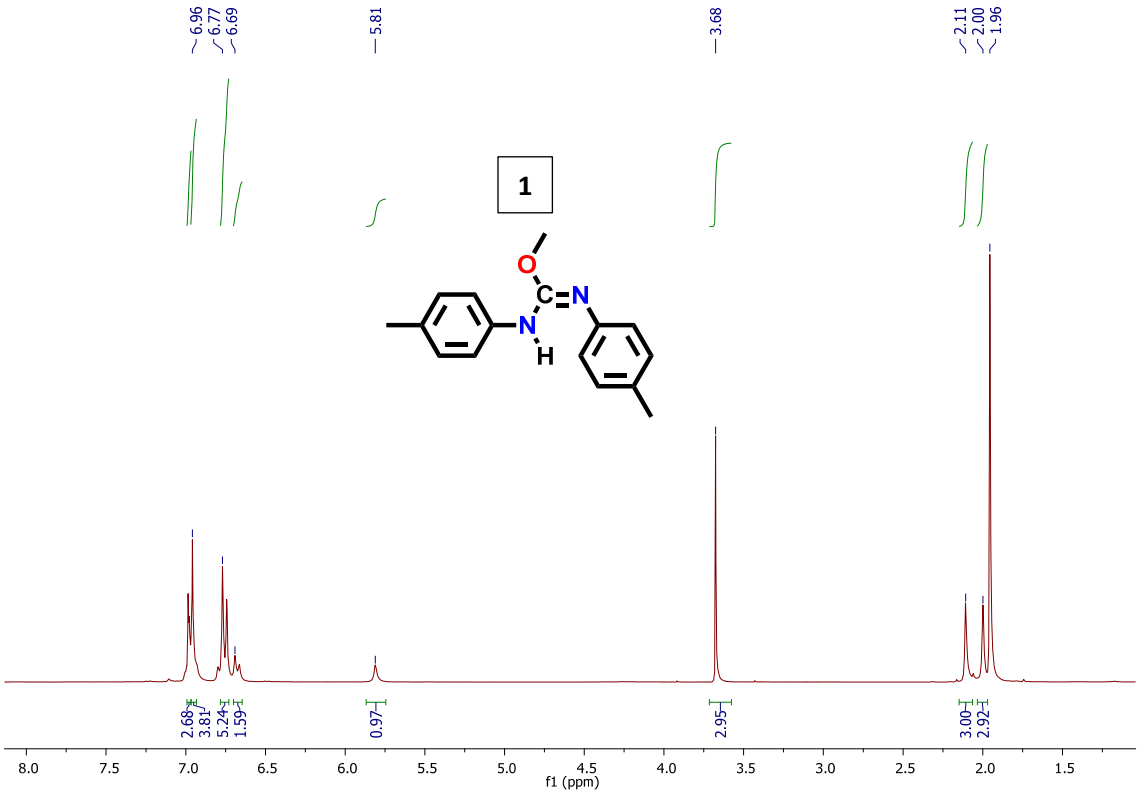

Figure S15. ^{1}H NMR of product 1.

3.2. Insertion of EtOH into di-p-tolylcarbodiimide with complex **1**

The insertion of ethanol (17.06 µL, 0.29 mmol) into di-p-tolylcarbodiimide (64.98 mg, 0.29 mmol) was carried out according to the general procedure described above.[1]H NMR (300 MHz, C_6D_6) δ 6.99 – 6.73 (m, 8H, *H*Ar), 5.84 (s,1H, N*H*), 4.30 (q , 1H, C*H*$_2$CH$_3$), 2.11 (s, 3H, C*H*$_3$), 2.00 (s, 3H, C*H*$_3$), 1.08 (t, 3H, CH$_2$C*H*$_3$).

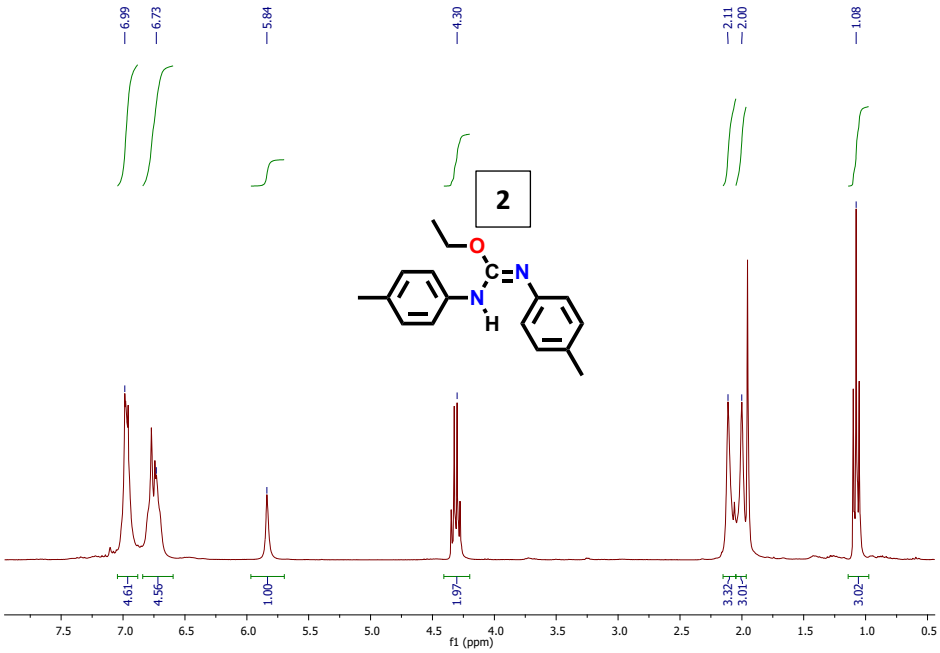

Figure S16. [1]H NMR of product 2.

3.3. Insertion of [i]PrOH into di-p-tolylcarbodiimide with complex **1**

The insertion of isopropanol (22.34 µL, 0.29 mmol) into di-p-tolylcarbodiimide (64.98 mg, 0.29 mmol) was carried out according to the general procedure described above. [1]H NMR (300 MHz, C_6D_6) δ 6.96 – 6.74 (m, 8H, *H*Ar), 5.83 (s, 1H, N*H*), 5.43 (m, 1H, C*H*(CH$_3$)$_2$), 2.11 (s, 3H, C*H*$_3$), 2.00 (s, 3H, C*H*$_3$), 1.19 (d, 6H, CH(C*H*$_3$)$_2$)

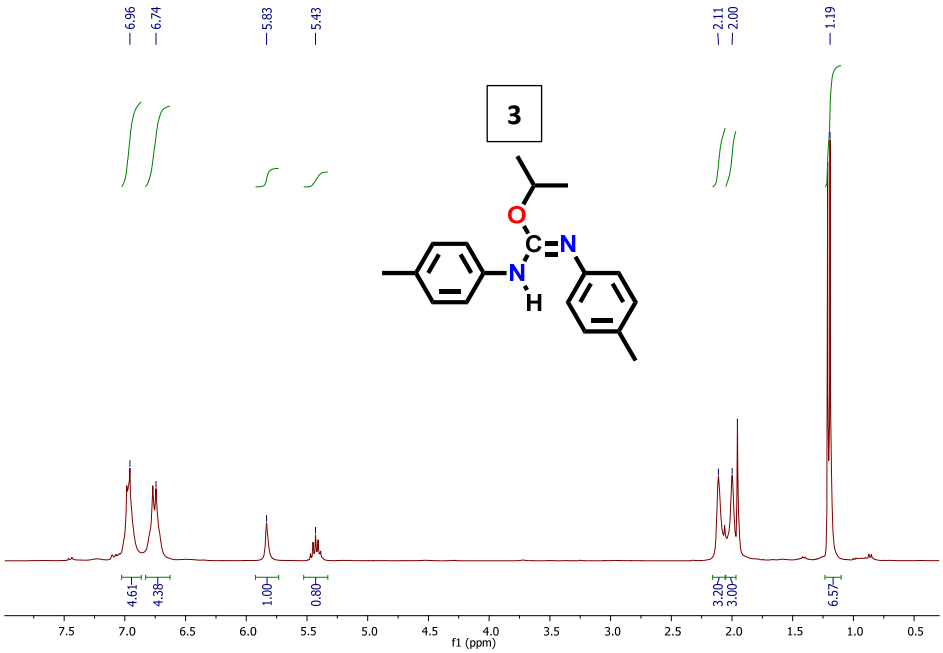

Figure S17. ^{1}H NMR of product 3.

3.4. Insertion of 1-Propanol into di-p-tolylcarbodiimide with complex **1**

The insertion of 1-propanol (21.87 µL, 0.29 mmol) into di-p-tolylcarbodiimide (64.98mg, 0.29 mmol) was carried out according to the general procedure described above. ^{1}H NMR (300 MHz, C_6D_6) δ 6.98 – 6.74 (m, 8H, *H*Ar), 5.85 (s,1H, N*H*), 4.25 (t , 2H, C*H*$_2$CH$_3$), 2.11 (s, 3H, C*H*$_3$), 2.00 (s,3H, C*H*$_3$), 1.53 (m, 2H, C*H*$_2$CH$_3$), 0.78 (t, 3H, CH$_2$C*H*$_3$).

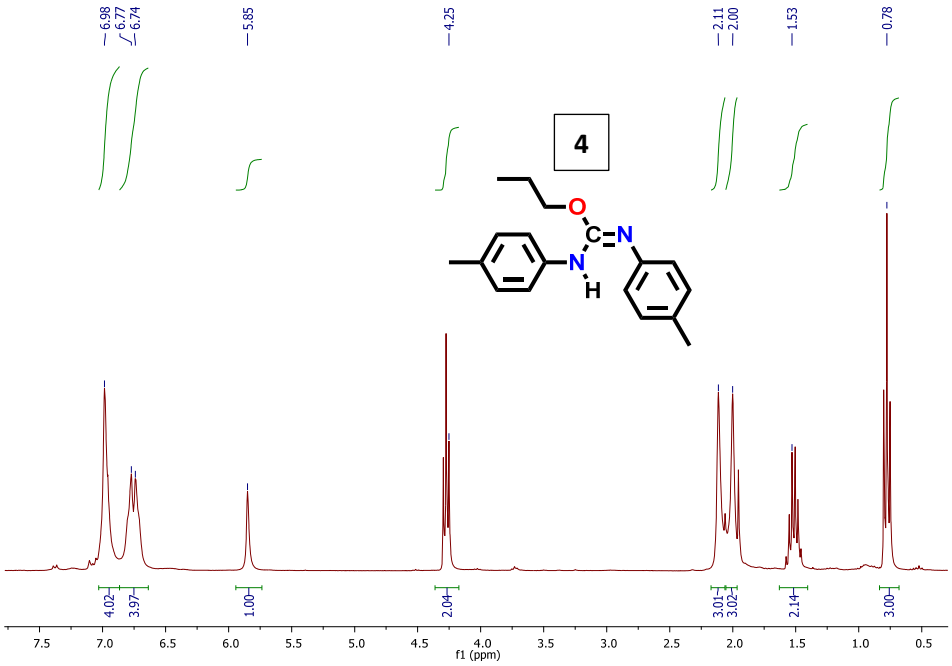

Figure S18. ^{1}H NMR of product 4.

3.5. Insertion of ^{t}BuOH into di-p-tolylcarbodiimide with complex **1**

The insertion of ^{t}BuOH (27.73 µL, 0.29 mmol) into di-p-tolylcarbodiimide (64.98 mg, 0.29 mmol) was carried out according to the general procedure described above. ^{1}H NMR (300 MHz, C_6D_6) δ 6.98 – 6.73 (m,8H, *H*Ar), 5.76 (s, 1H, N*H*), 2.11 (s, 3H, CH_3), 2.01 (s, 3H, CH_3), 1.55 (s, 9H, C(CH_3)$_3$).

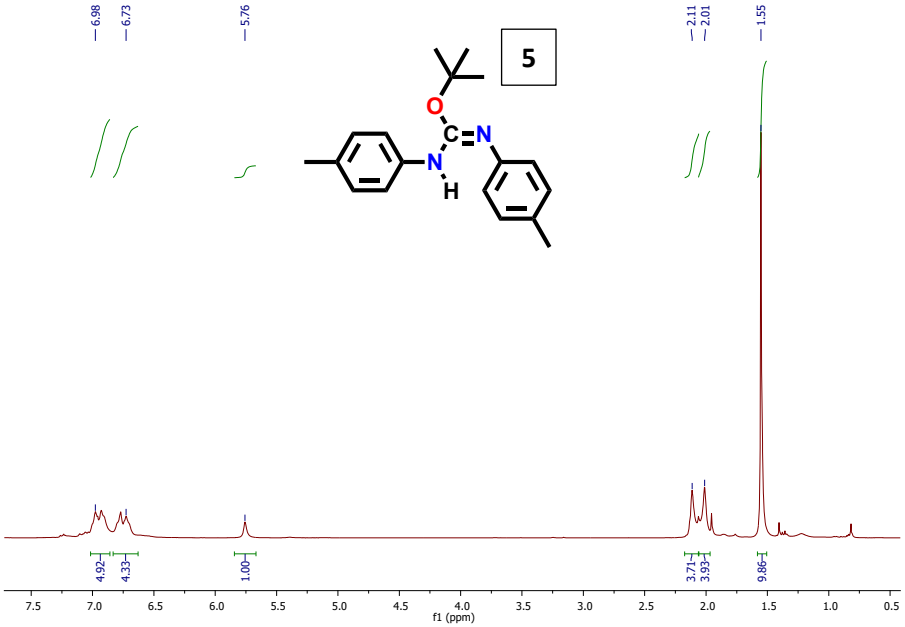

Figure S19. ^{1}H NMR of product 5.

3.6. Insertion of benzyl alcohol into di-p-tolylcarbodiimide with complex **1**

The insertion of benzylalcohol (30.28 µL, 0.29 mmol) into di-p-tolylcarbodiimide (64.98 mg, 0.29 mmol) was carried out according to the general procedure described above. ^{1}H NMR (300 MHz, C_6D_6) δ 6.96 – 6.71 (m, 8H, *H*Ar), 5.89 (s, 1H, N*H*), 5.40 (s, 2H, CH_2Ph), 2.11 (s, 3H, CH_3), 1.95 (s, 3H, CH_3).

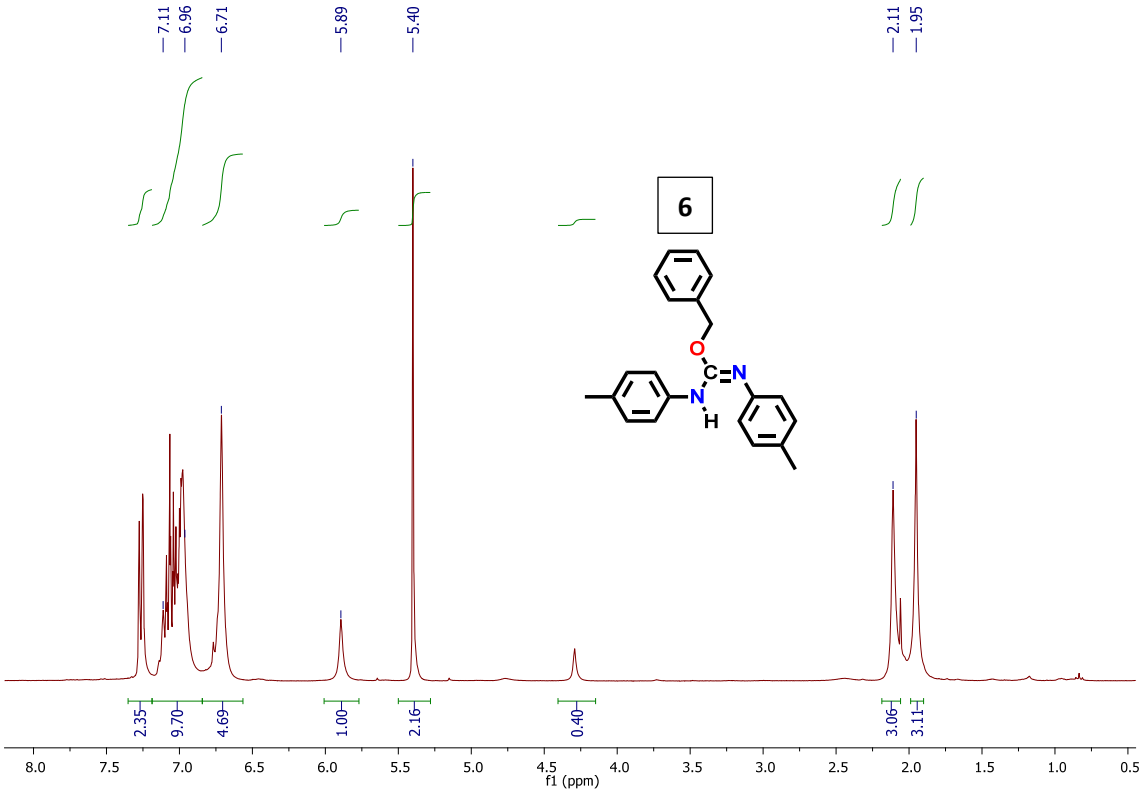

Figure S20. ^{1}H NMR of product 6.

3.7. Insertion of 4-tertbutylphenol into di-p-tolylcarbodiimide with complex **1**

The insertion of 4-tertbutylphenol (43.91 mg, 0.29 mmol) into di-p-tolylcarbodiimide (64.98 mg, 0.29 mmol) was carried out according to the general procedure described above. ^{1}H NMR (300 MHz, C_6D_6) δ 7.10 – 6.58 (m, 13H, *H*Ar, N*H*), 2.02 (s, 6H, CH_3), 1.08 (s, 9H, C(CH_3)$_3$)

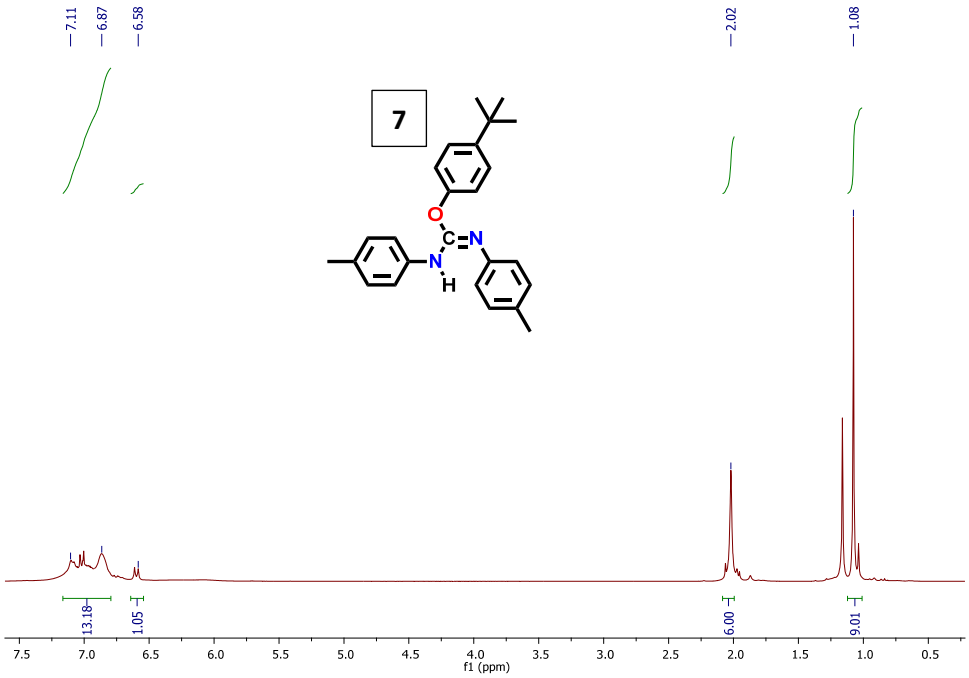

Figure S21. ^{1}H NMR of product 7.

3.8. Insertion of 4-methylphenol into di-p-tolylcarbodiimide with complex **1**

The insertion of 4-methylphenol (31.61 mg, 0.29 mmol) into di-p-tolylcarbodiimide (64.8 mg, 0.29 mmol) was carried out according to the general procedure described above. ^{1}H NMR (300 MHz, C_6D_6) δ 7.10 – 6.77 (m, 13H, *H*Ar, N*H*), 2.07 (s, 6H, C*H*$_3$), 2.03 (s, 3H, C*H*$_3$).

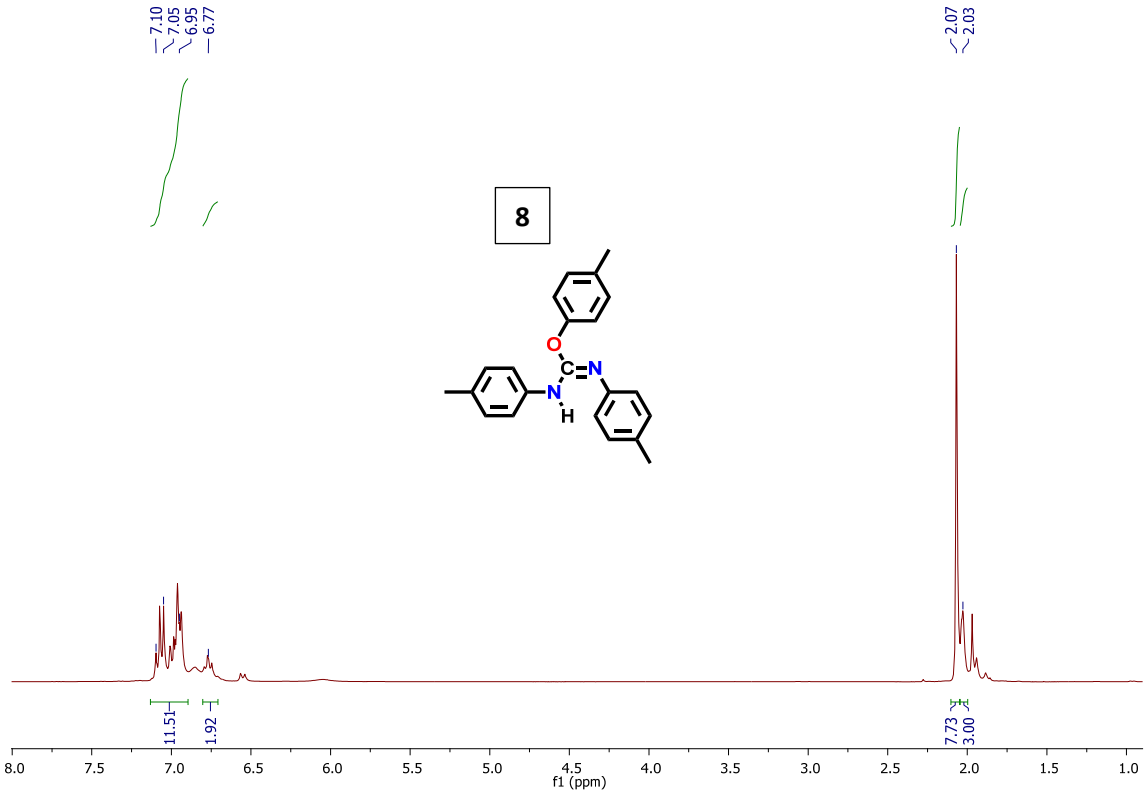

Figure S22. ^{1}H NMR of product 8.

3.9. Insertion of 4-flourolphenol into di-p-tolylcarbodiimide with complex **1**

The insertion of 4-flourophenol (32.78 mg, 0.29 mmol) into di-p-tolylcarbodiimide (64.98 mg, 0.29 mmol) was carried out according to the general procedure described above. ^{1}H NMR (300 MHz, C_6D_6) δ 7.10 – 6.75 (m, 13H, *H*Ar, N*H*), 2.07 (s, 6H, C*H*$_3$)

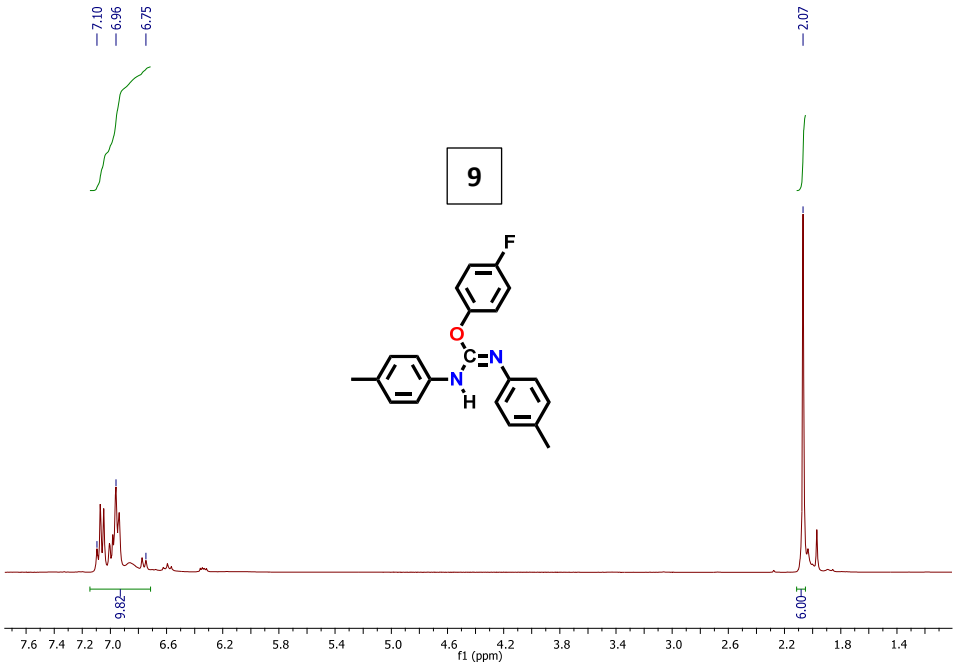

Figure S23. ^{1}H NMR of product 9.

3.10. Insertion of 2,6-methylphenol into di-p-tolylcarbodiimide with complex **1**

The insertion of 2,6-dimethylphenol (35.71 mg, 0.29 mmol) into di-p-tolylcarbodiimide (64.98 mg, 0.29 mmol) was carried out according to the general procedure described above. ^{1}HNMR (300 MHz, C_6D_6) δ6.99 – 6.74 (m, 11H, *H*Ar), 5.90 (brs, 1H, N*H*), 2.25 (s, 6H, C*H*$_3$), 2.06 (s, 3H, C*H*$_3$), 2.04 (s, 3H, C*H*$_3$).

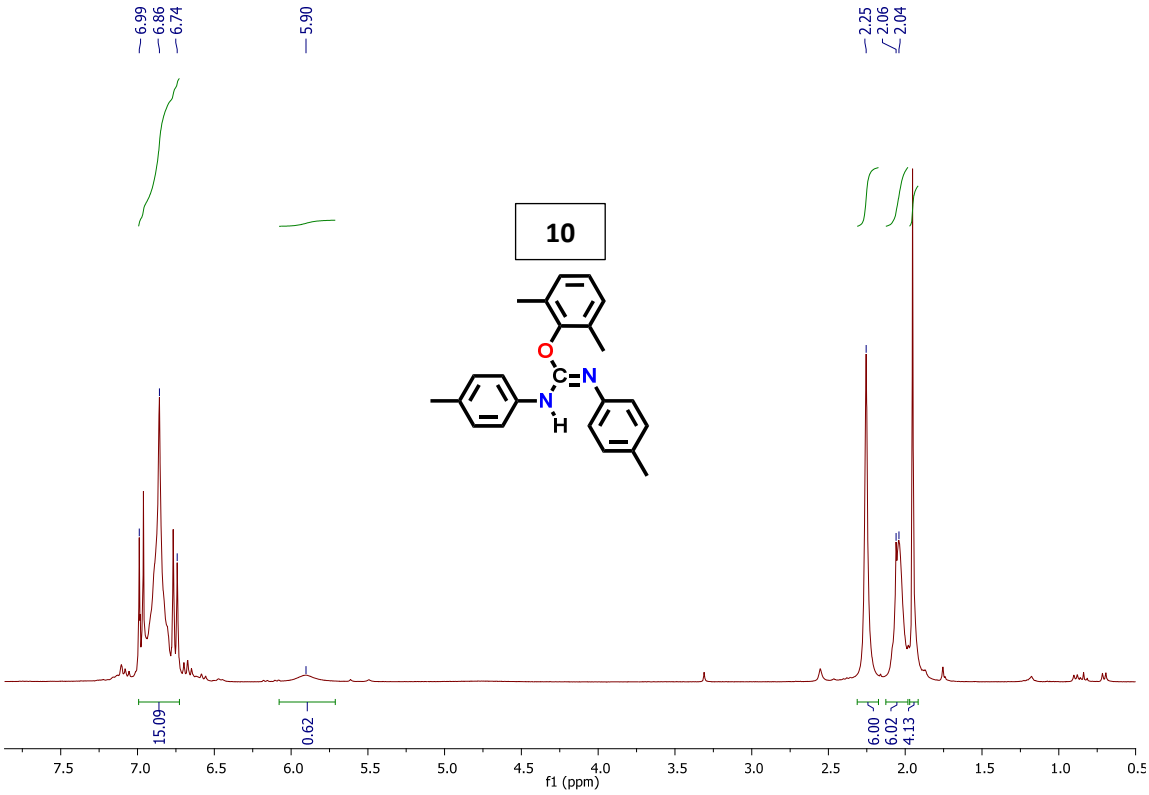

Figure S24. ^{1}H NMR of product 10.

3.11. Insertion of phenol into di-p-tolylcarbodiimide with complex **1**

The insertion of phenol (27.51 mg, 0.29 mmol) into di-p-tolylcarbodiimide (64.98 mg, 0.29 mmol) was carried out according to the general procedure described above. ^{1}H NMR (300 MHz, C_6D_6) δ 7.10 – 6.58 (m, 14H, *H*Ar, N*H*), 2.07 (s, 6H, C*H*$_3$).

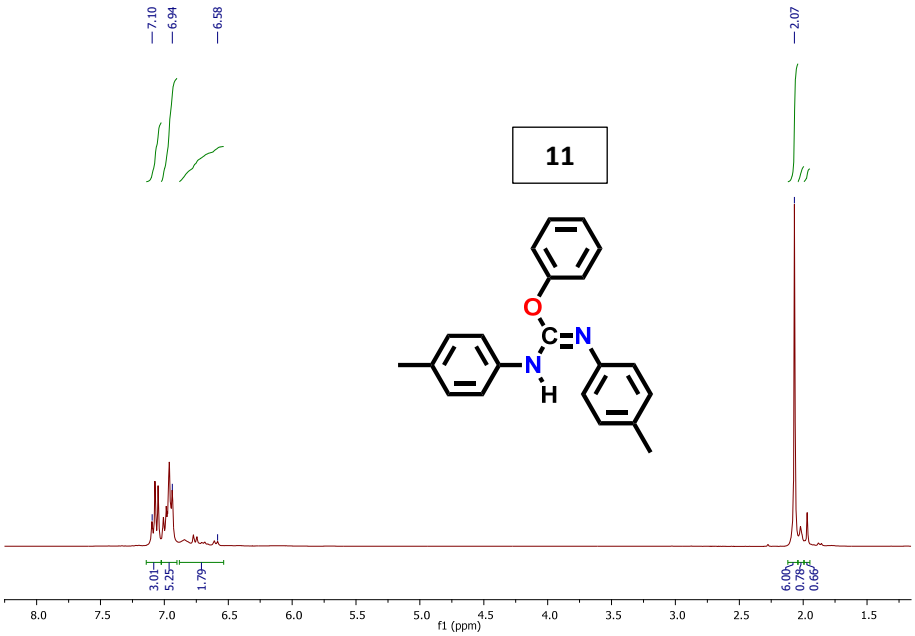

Figure S25. ^{1}H NMR of product 11.

3.12. Insertion of 3,5-ditertbutylphenol into di-p-tolylcarbodiimide with complex **1**

The insertion of 3,5-ditertburtylphenol (60.3 mg, 0.29 mmol) into di-p-tolylcarbodiimide (64.98 mg, 0.29 mmol) was carried out according to the general procedure described above. This reaction did not work, and here are only the starting reagents. ^{1}H NMR (300 MHz, C_6D_6) δ 7.32-6.08 (m, 11H, *H*Ar, 1.96 (s, 6H, C*H*$_3$), 1.48 (s, 9H, C(C*H*$_3$)), 1.23(s, 9H, C(C*H*$_3$)).

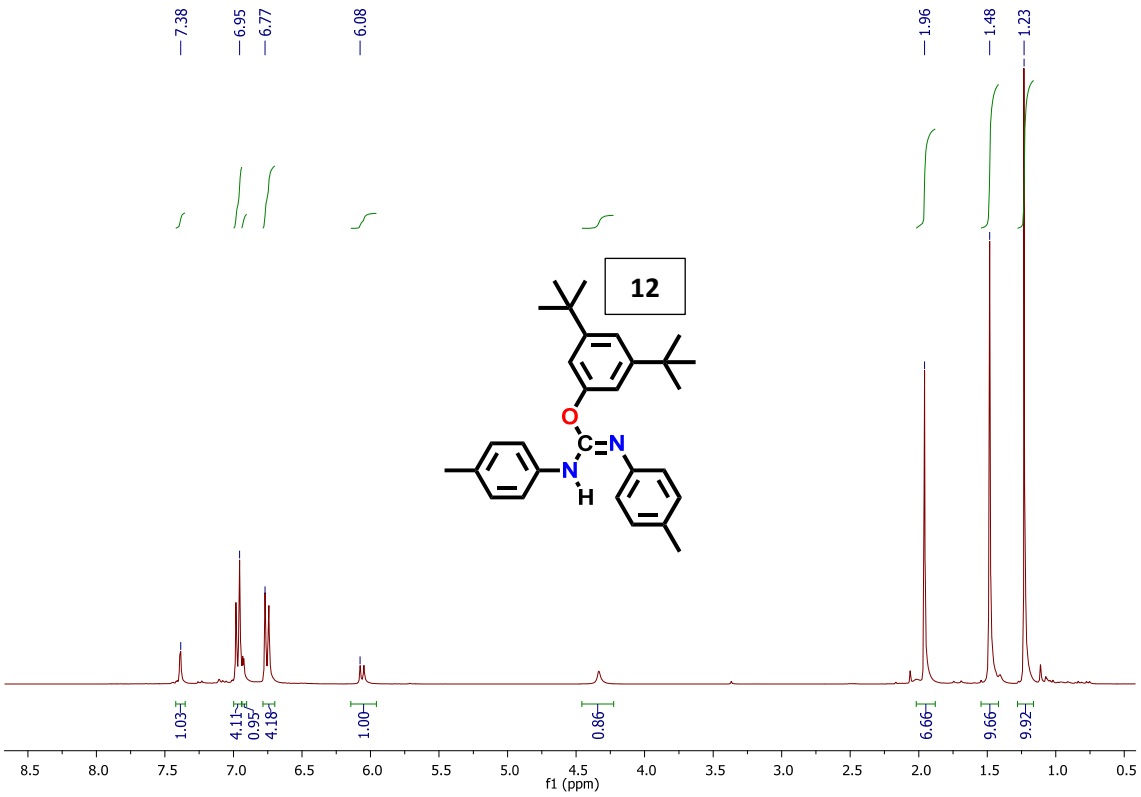

Figure S26. ^{1}H NMR of product 12.

3.13. Insertion of MeOH into di-o-tolylcarbodiimide with complex **1**

The insertion of MeOH (11.82 µL, 0.29 mmol) into di-o-tolylcarbodiimide (64.98 mg, 0.29 mmol) was carried out according to the general procedure described above. ^{1}H NMR (300 MHz, C_6D_6) δ 6.96 (m, 4H, HAr), 6.77-6.66(m, 4H, HAr), 5.81 (s, 1H, NH), 3.67(s, 3H, CH_3), 2.00 (d, 6H, CH_3). ^{13}C NMR (100 MHz, C_6D_6) δ 148.41, 143.91, 134.25, 130.09, 129.66, 128.26, 127.13, 120.53, 118.71, 51.24, 18.41, 18.24.

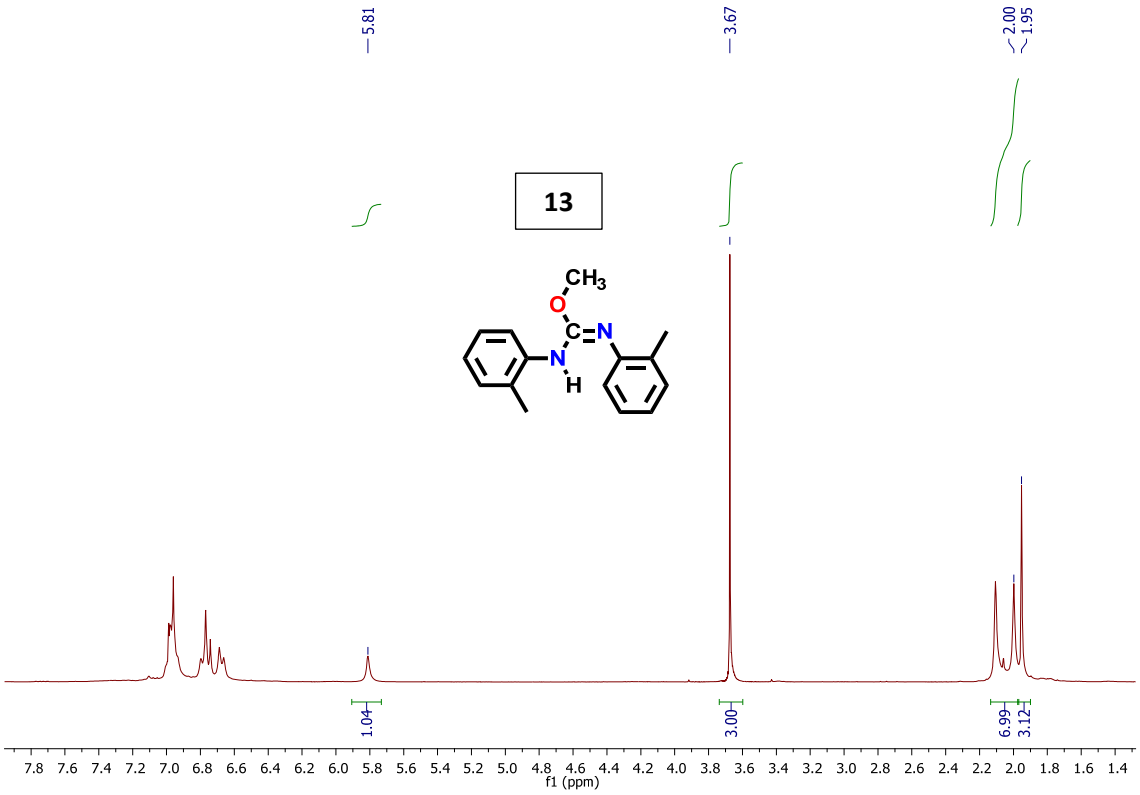

Figure S27. ^{1}H NMR of product 13.

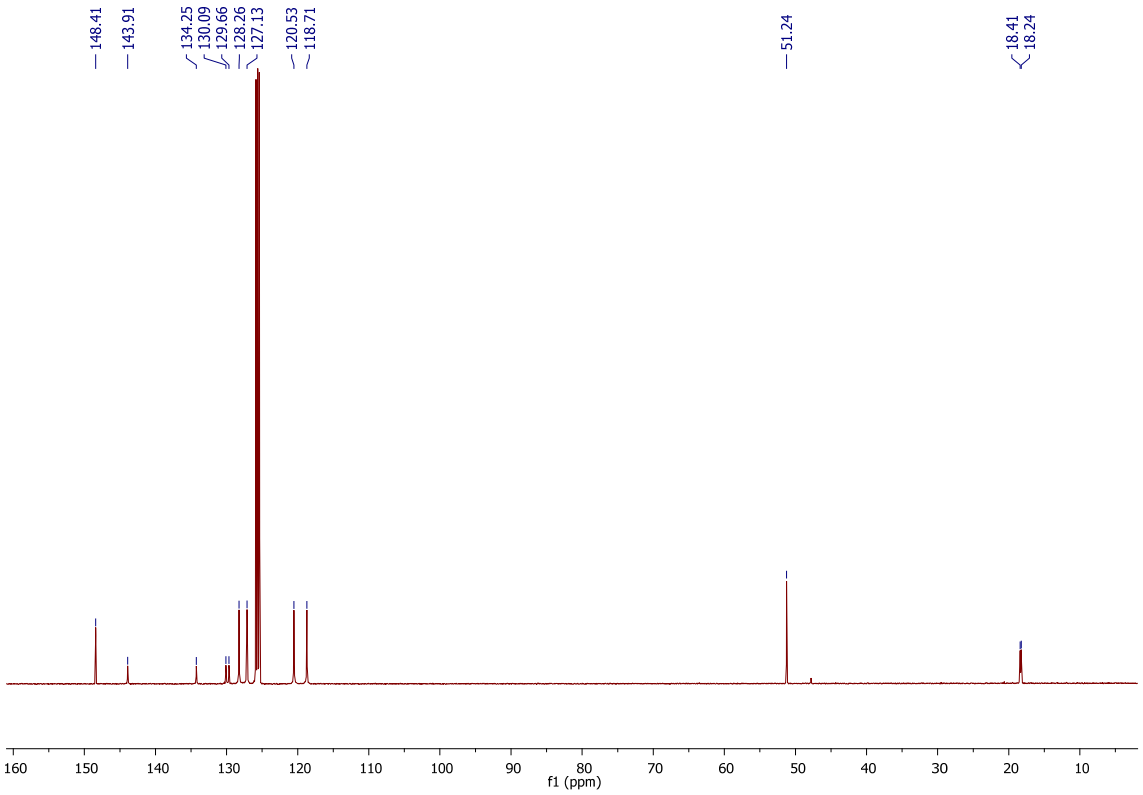

Figure S28. ^{13}C NMR of product 13.

3.14. Insertion of MeOH into N-(2,4,6-trimethylphenyl)-N'-phenyl-carbodiimide with complex **1**

The insertion of MeOH (11.82 µL, 0.29 mmol) into carbodiimide (69.17 mg, 0.29 mmol) was carried out according to the general procedure described above. The NMR is of the major product. ^{1}H NMR (300 MHz, C_6D_6) δ 6.97(m, 3H, HAr), 6.70(d, 2H, HAr), 6.62(s, 2H, HAr), 5.53(s, 1H, NH), 3.77(s, 3H, CH_3), 2.25(s, 6H, CH_3), 2.07(s, 3H, CH_3). ^{13}C NMR (100 MHz, C_6D_6) δ 149.65, 146.61, 140.16, 136.60, 133.79, 129.54, 127.57, 127.23, 126.54, 120.66, 118.38, 51.28, 18.49, 15.83.

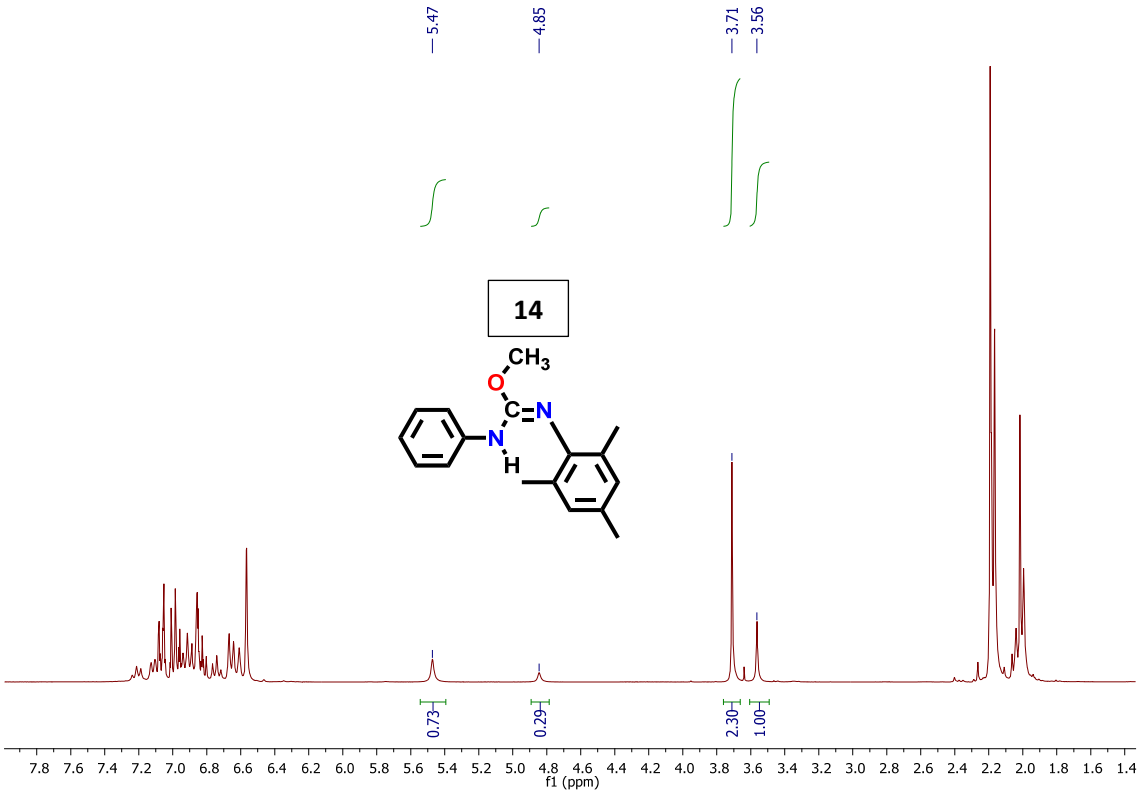

Figure S29. ^{1}H NMR of product 14.

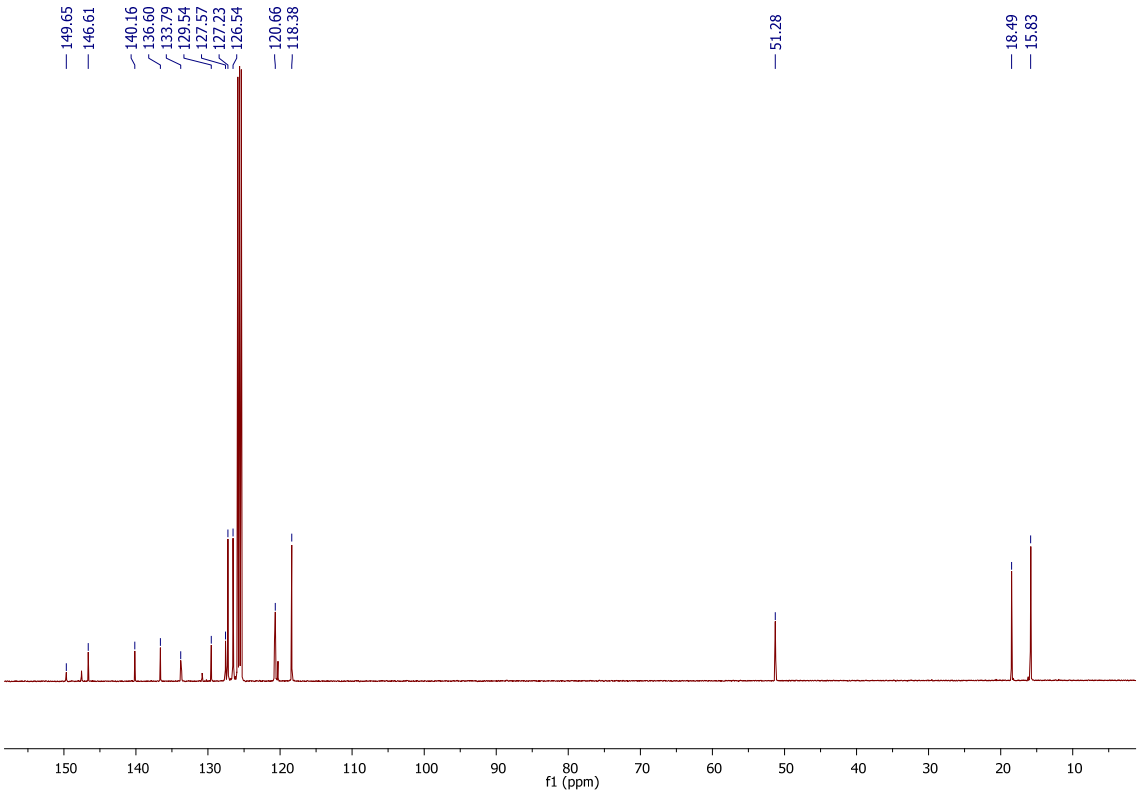

Figure S30. ^{13}C NMR of product 14.

3.15. Insertion of MeOH into 2,6-bis-isopropyl-N-(phenylcarbonimidoyl)aniline with complex **1**

The insertion of MeOH (11.82 µL, 0.29 mmol) into carbodiimide (81.5 mg, 0.29 mmol) was carried out according to the general procedure described above. The NMR is of the major product. ^{1}H NMR (300 MHz, C_6D_6) δ 6.97(m, 3H, HAr), 6.91(m, 2H, HAr), 6.74(t, 1H, HAr), 6.66(d, 2H, HAr), 5.53(s, 1H, NH), 3.71(s, 3H, CH_3), 3.22(q, 2H, $CH(CH_3)_2$), 1.21-1.18(d, 12H, CH_3). ^{13}C NMR (100 MHz, C_6D_6) δ 146.43, 140.19, 138.10, 136.39, 126.56, 121.72, 121.68, 120.80, 118.46, 51.33, 26.19, 21.34.

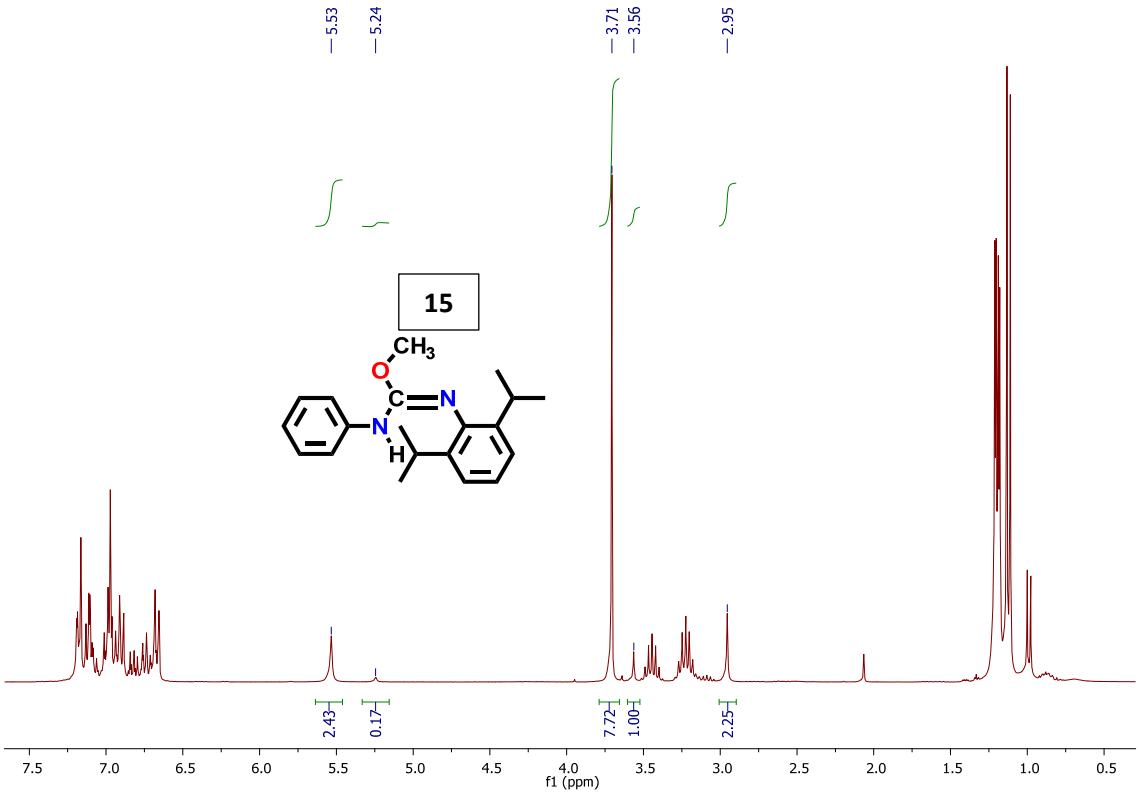

Figure S31. ^{1}H NMR of product 15.

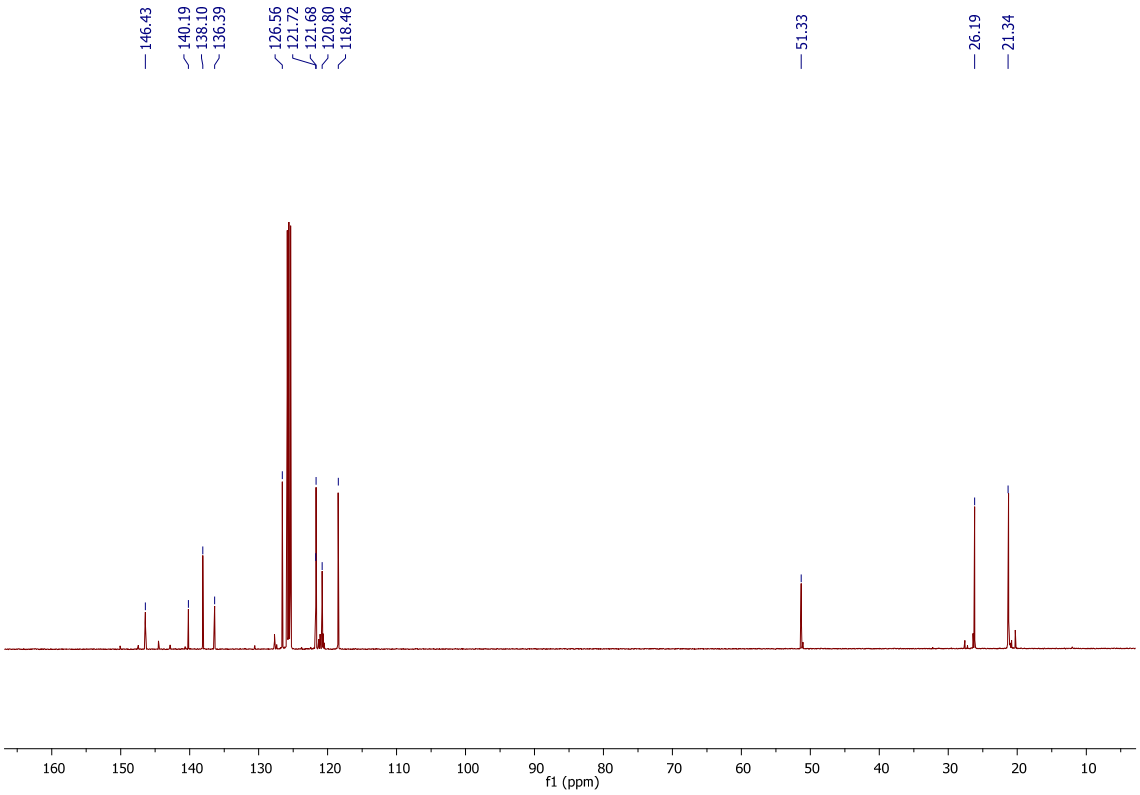

Figure S32. ^{13}C NMR of product 15.

3.16. Insertion of MeOH into N,N'-bis(4-methoxyphenyl)carbodiimide with complex **1**
The insertion of MeOH (11.82 µL, 0.29 mmol) into carbodiimide (74.4 mg, 0.29 mmol) was carried out according to the general procedure described above. ^{1}H NMR (300 MHz, C_6D_6) δ 6.95(d, 2H, HAr), 6.80(d, 2H, HAr), 6.70(d, 2H, HAr), 6.56(d, 2H, HAr), 5.75(s, 1H, NH), 3.69(s, 3H, CH_3), 3.22(s, 3H, CH_3).

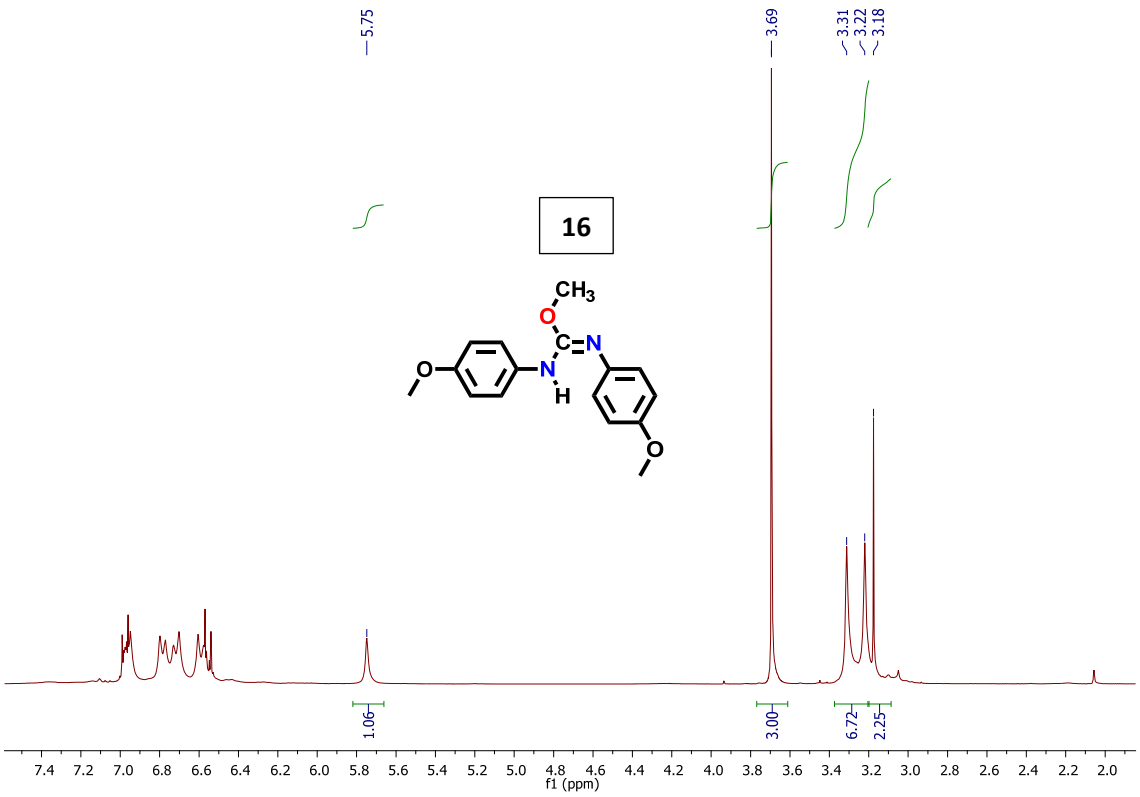

Figure S33. ^{1}H NMR of product 16.

4. Kinetic studies of MeOH into DTC using complex **1**

All the kinetic experiments were done in the following procedure. A J. Young NMR tube was charged with a pre-prepared solution of DTC, MeOH, complex in C_6D_6, and a total volume of 0.6 mL. The solution was added in the glove box and then the tube was sealed. The NMR tube was taken out of the glove box and the ^{1}H NMR experiment began at 25°C. All the experiments were done by changing only one of the substrates or the complex while other reagents were constant, and the data was collected every several minutes. The product concentrations were measured by the area ratio of the methyl group at 3.0ppm and 3.7 ppm, which were assigned to the starting material and product respectively. Reaction rates were determined by the least-square fit of the initial product concentration versus time, and the plots were shown in Figures S1-3.

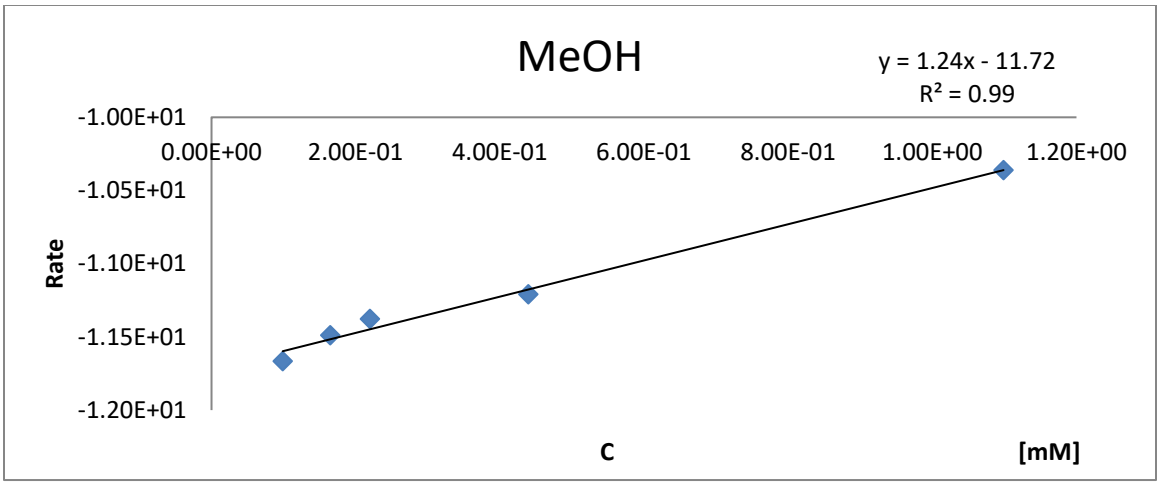

Figure S34. The plot of reaction rate versus concentration of MeOH catalyzed by complex **1**

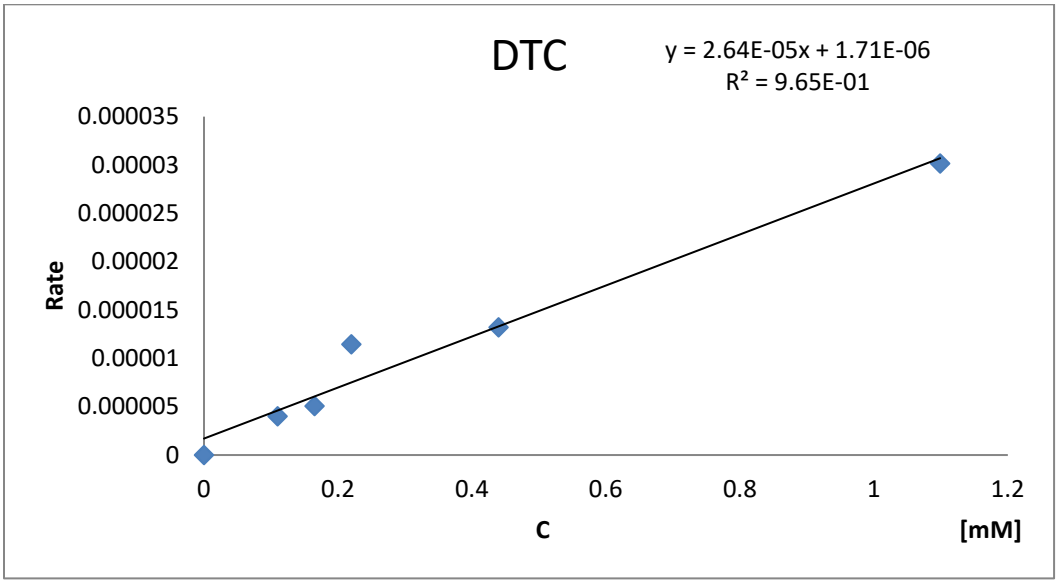

Figure S35. The plot of reaction rate versus concentration of DTC catalyzed by complex **1**

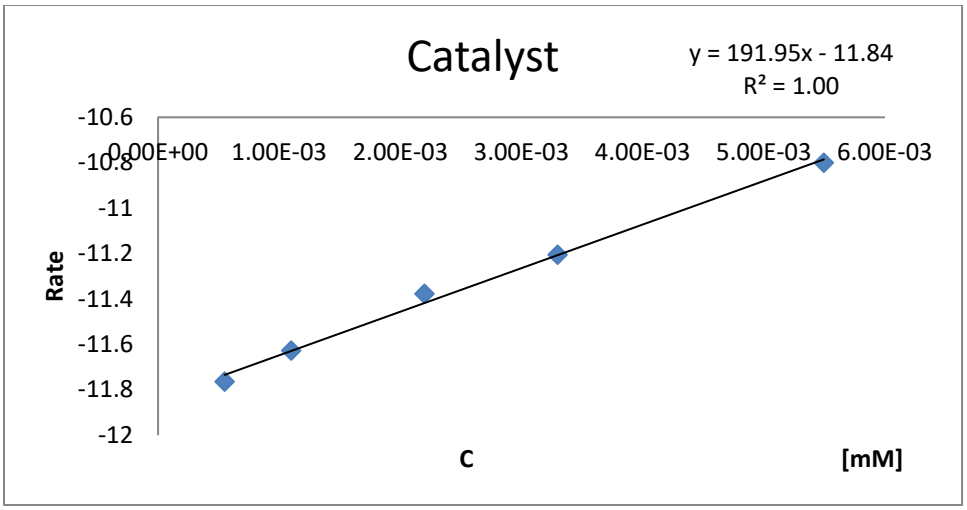

Figure S36. The plot of reaction rate versus concentration of catalyst **1** while DTC and MeOH are constant.

Activation parameters of enthalpy ($\Delta H^{\ddagger}$), entropy ($\Delta S^{\ddagger}$) and activation energy (Ea) were calculated from the kinetic data using Eyring and Arrhenius plots. The procedure is similar to the one mentioned previously, a J. Young tube was loaded with complex **1**, DTC, and MeOH. Then the sample was submerged into an oil bath preheated to a constant temperature set and measured for ^{1}HNMR. Several NMR tubes were measured at different temperatures at the same reaction time. The data was collected by measuring ^{1}H NMR. Reaction rates were determined by the least square fit of initial product concentration versus time, and Eyring and Arrhenius's plots were shown in Figures S37-38. Enthalpy ($\Delta H^{\ddagger}$), entropy ($\Delta S^{\ddagger}$) and activation energy (Ea) were calculated from the slope and intercept of the least-square fit.

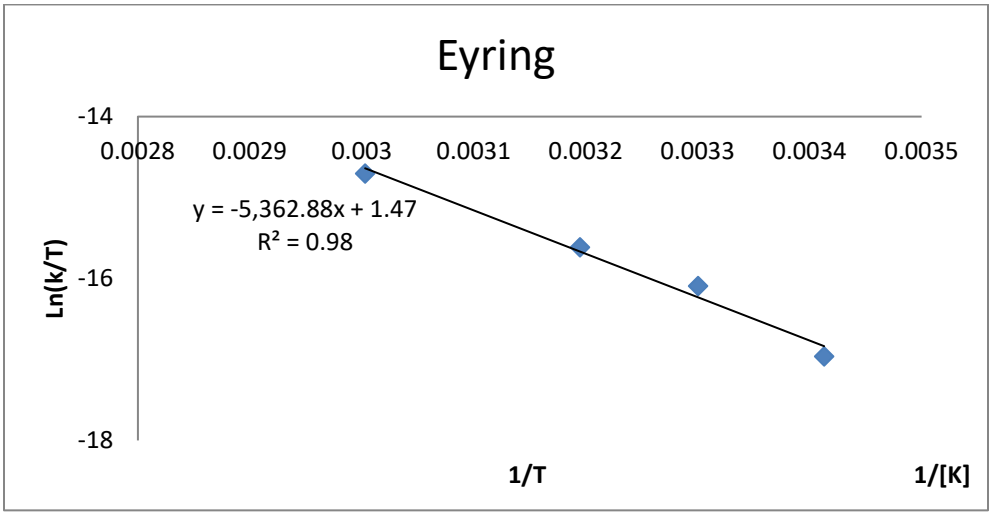

Figure S37. Eyring plot for the reaction of DTC and MeOH using complex **1**

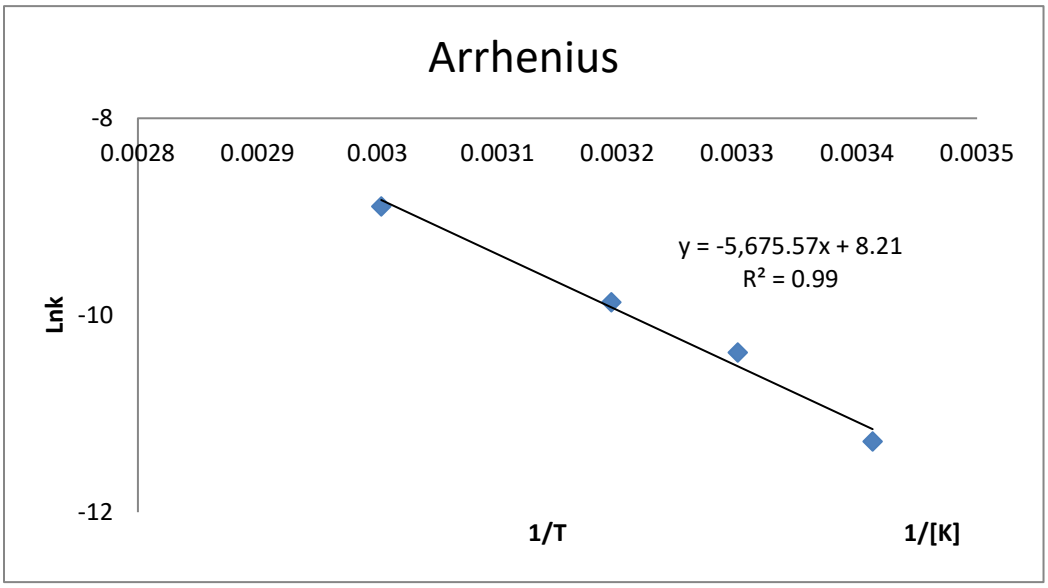

Figure S38. Arrhenius plot for the reaction of DTC and MeOH using complex **1**

The following mechanism was proposed as a result of the data gathered.

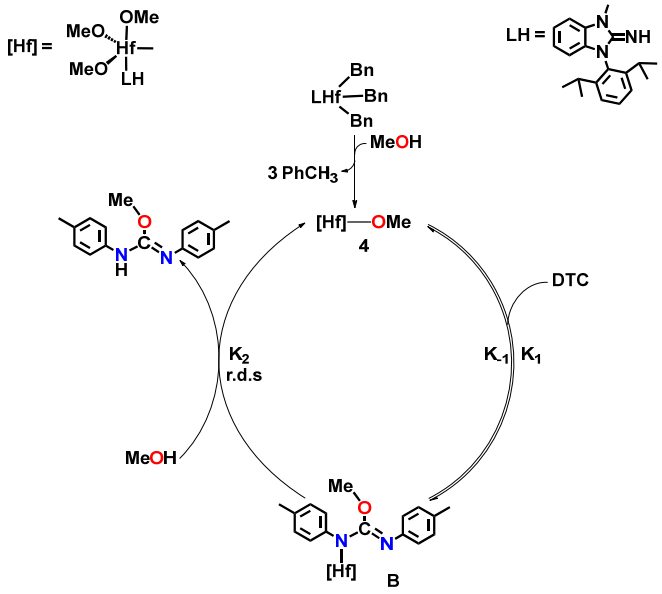

Figure S39. A plausible mechanism for the reaction of DTC and MeOH using complex **1**

5. Kinetic isotopic effect of MeOH and MeOD with complex **1**

All the KIE experiments were performed charging a J. Young NMR tube with complex **1**, DTC, MeOH, or ^{t}BuOH and adding C_6D_6 until a total volume of 0.6mL in a glove box. The experiments were measured at 25°C following the ^{1}H NMR signals. The product concentration was measured by the area ratio of the MeOH group at 3.0ppm and 3.7 ppm, which were assigned to the starting material and product respectively. Reaction rates were determined by the least-square fit of the initial product concentration versus time, and the plots were shown in Figures S6. The KIE value was calculated from the ratio of the two slopes. The KIE measurements were done and then we have appreciated that the KIE = 2.78.

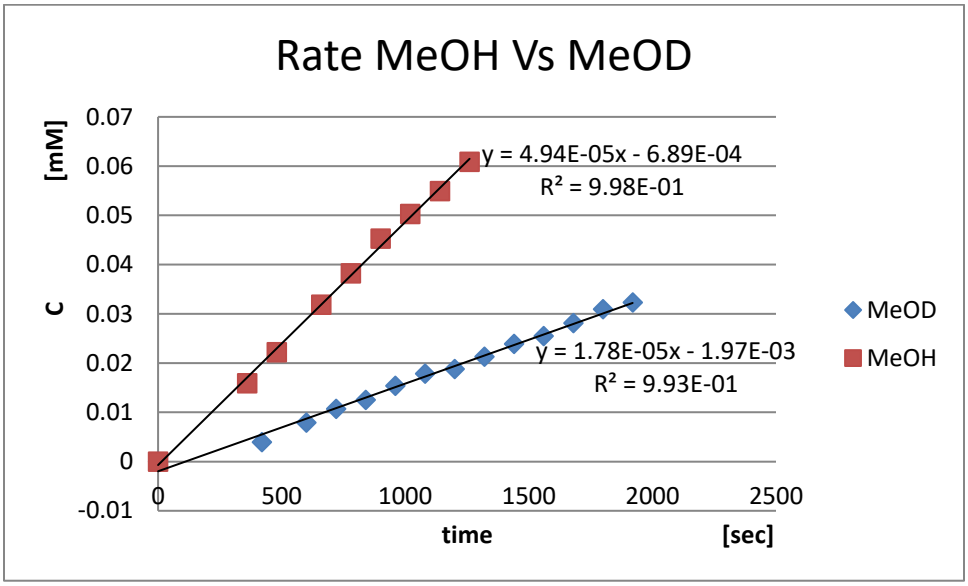

Figure S40. Plot for the reaction of DTC and MeOH and MeOD using complex **1**

6. Kinetic isotopic effect of ^{t}BuOH and ^{t}BuOD with complex **1**

The product concentration was measured by the area ratio of the ^{t}BuOH group at 1.03ppm and 1.55ppm, which were assigned to the starting material and product respectively. Reaction rates were determined by the least-square fit of the initial product concentration versus time, and the plots were shown in Figures S41. The KIE value was calculated from the ratio of the two slopes. The KIE measurements were done and then we have appreciated that the KIE = 1.31.

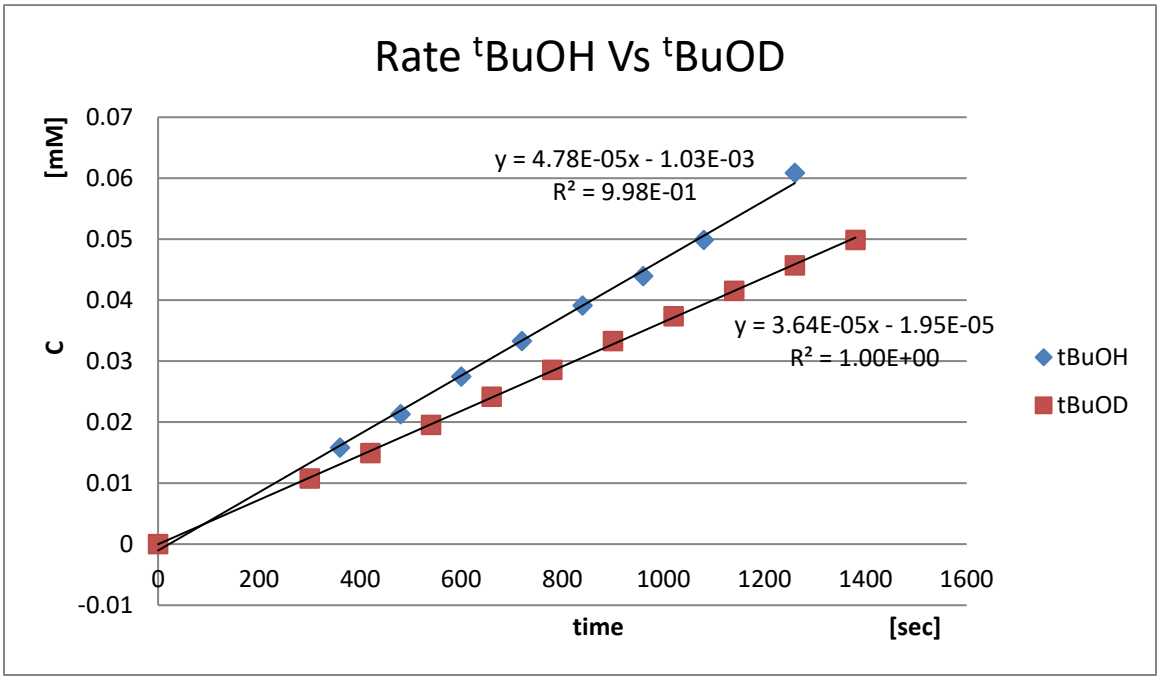

Figure S41. Plot for the reaction of DTC and MeOH and MeOD using complex **1**

6.1. The reaction between complex **1** and 4 equiv of ^{t}BuOD

An experiment to check the appearance of NH moiety of complex **4** was done, in this experiment we made a reaction between complex **1** and 4equiv of ^{t}BuOD, the following ^{1}HNMR shows that the signal at 5.22 ppm disappeared.

^{1}H NMR (300 MHz, C_6D_6) δ 7.06(m, 18H, *H*-Ph) , 6.81(t, 1H,*H*-Ar), 6.70 (t, 1H,*H*-Ar), 6.53 (d, 1H,*H*-Ar), 6.14 (d, 1H,*H*-Ar), 3.74 (s, 3H, C*H*$_3$), 2.63 (m, 2H, C*H*(CH$_3$)$_2$), 2.04 (DC*H*$_2$-Ph), 1.34(s, 36H, CC*H*$_3$), 1.19(d, 6H, CH(C*H*$_3$)$_2$), 0.81(d, 6H, CH(C*H*$_3$)$_2$).

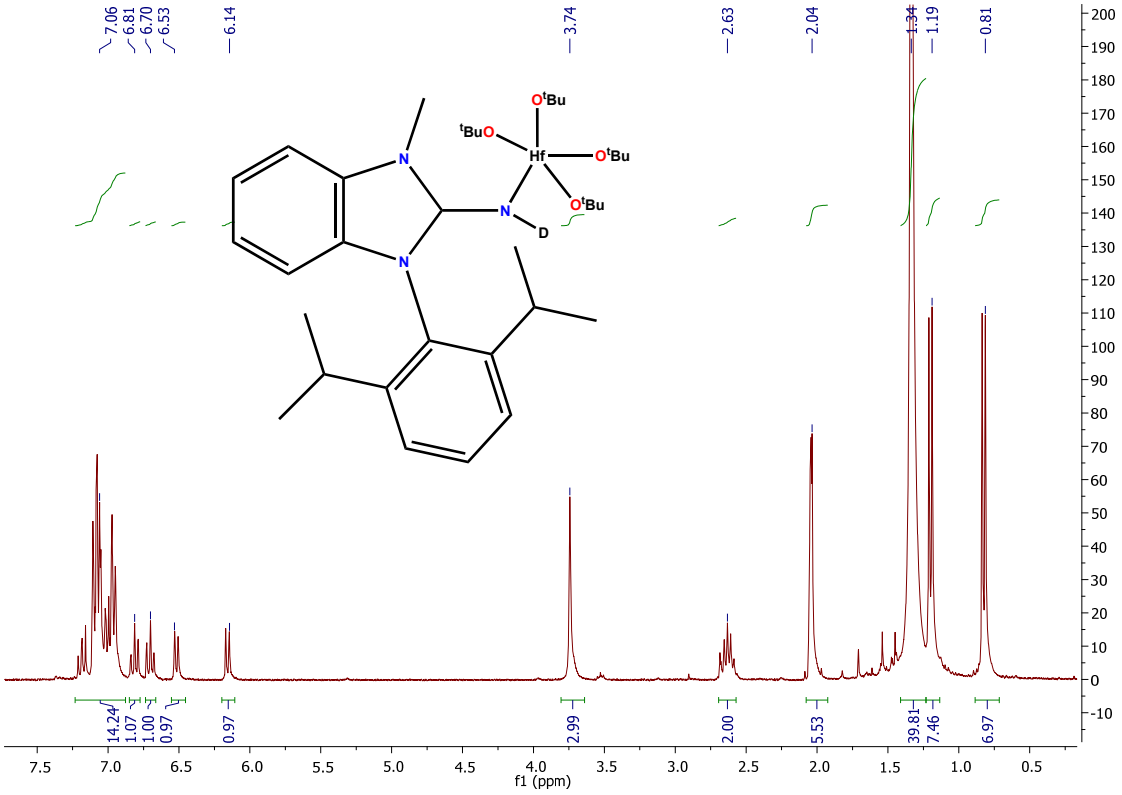

Figure S42. Reaction of complex **1** with 4equiv of ^{t}BuOD

7. Stoichiometric reactions

All the stoichiometric experiments were done in a similar method. A J. Young NMR tube was loaded with complex **1** and 1equiv or 4equiv of ^{t}BuOH and/or DTC, diluted to a total volume of 600 µL by C_6D_6 and monitored by ^{1}H NMR spectroscopy.

7.1. Hafnium tetrabenzyl

The following complex was prepared according to a known procedure. [3]

^{1}H NMR (300 MHz, C_6D_6) δ 7.04(t, 8H, Ar), 6.89(t, 4H, Ar), 6.47(d, 8H, Ar, 1.44(s, 8H, CH_2).

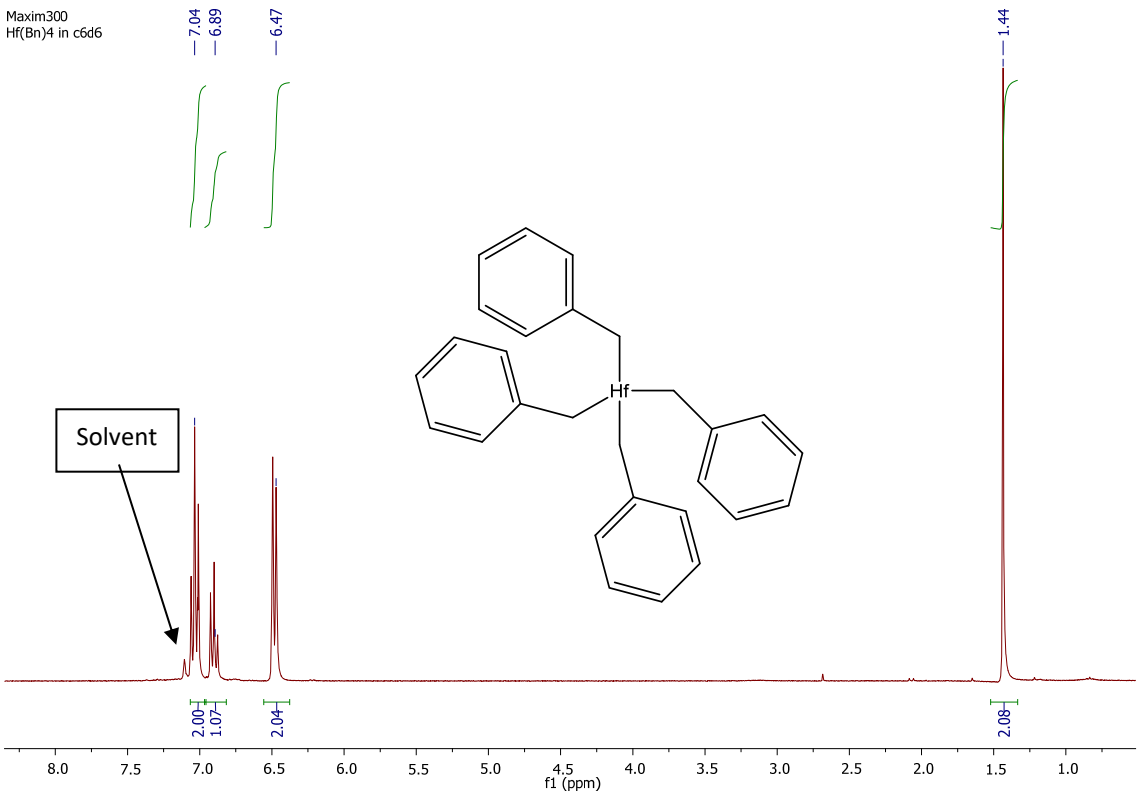

Figure S43. ^{1}H NMR of hafnium tetrabenzyl.

7.2. Addition of ^{t}BuOH to hafnium tetrabenzyl

5equiv of ^{t}BuOH was added to a solution of 1equiv hafnium tetrabenzyl complex and monitored by ^{1}HNMR. Formation of toluene can be seen at 2.1ppm and no benzyls are left.

^{1}H NMR (300 MHz, C_6D_6) δ 7.11-6.95(m, 5H, *H*-Ar), 2.06(s, 3H, CH_3), 1.21(s, 9H, CH_3).

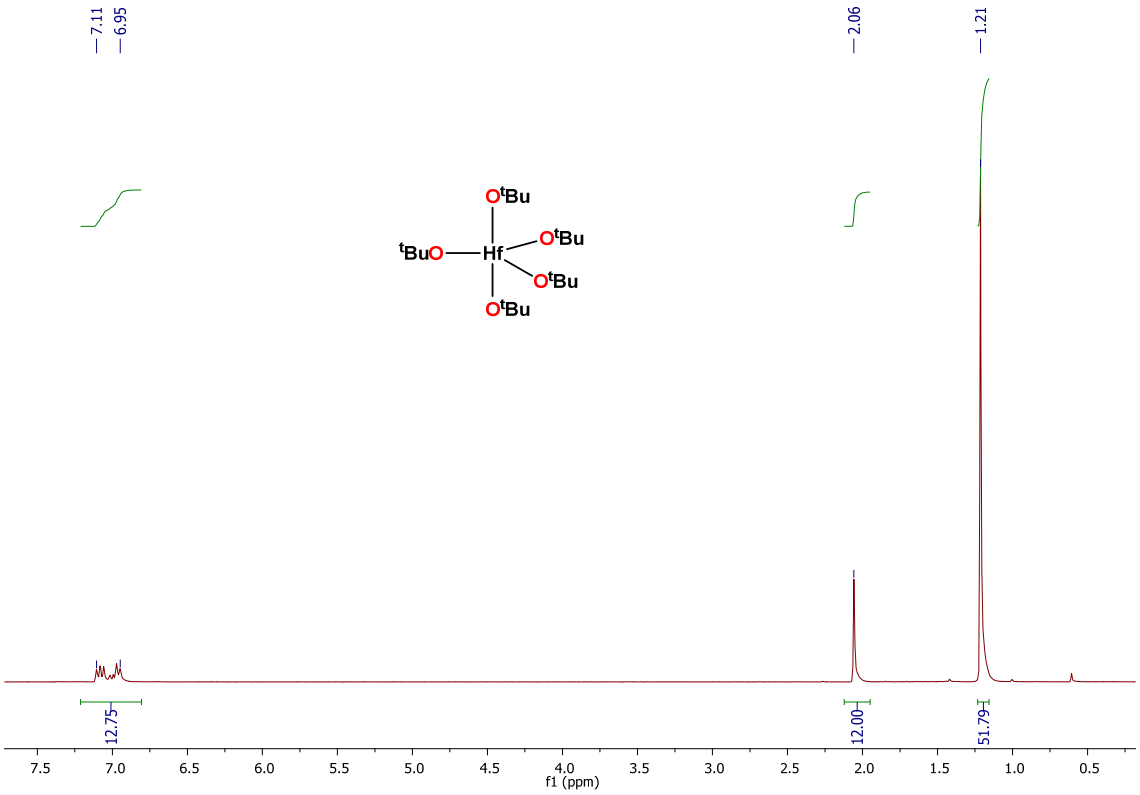

Figure S44. ^{1}H NMR of hafnium tetrabenzyl reaction with ^{t}BuOH.

7.3. Addition of DTC to the homoleptic tertbutoxide hafnium complex

1 equiv of DTC solution was added to a solution of homoleptic tertbutoxide hafnium complex and monitored by ^{1}HNMR. The signal at 2.06 is an indication for the formation of toluene as the benzyls leave. All the starting DTC was consumed turning to the signal at 2.13ppm. Formation of a new signal at 1.50 ppm which is the new ^{t}BuOH signal shifted on the amidinate is formed.

^{1}H NMR (300 MHz, C_6D_6) δ 7.27-6.72 (m, 28H, *H*-Ar), 5.76 (brs, 1H, N-*H*), 2.13 (s, 3H, C*H*$_3$), 1.50 (s, 9H, C*H*$_3$), 1.41 (s, 3H, C*H*$_3$), 1.25 (s, 27H, C*H*$_3$).

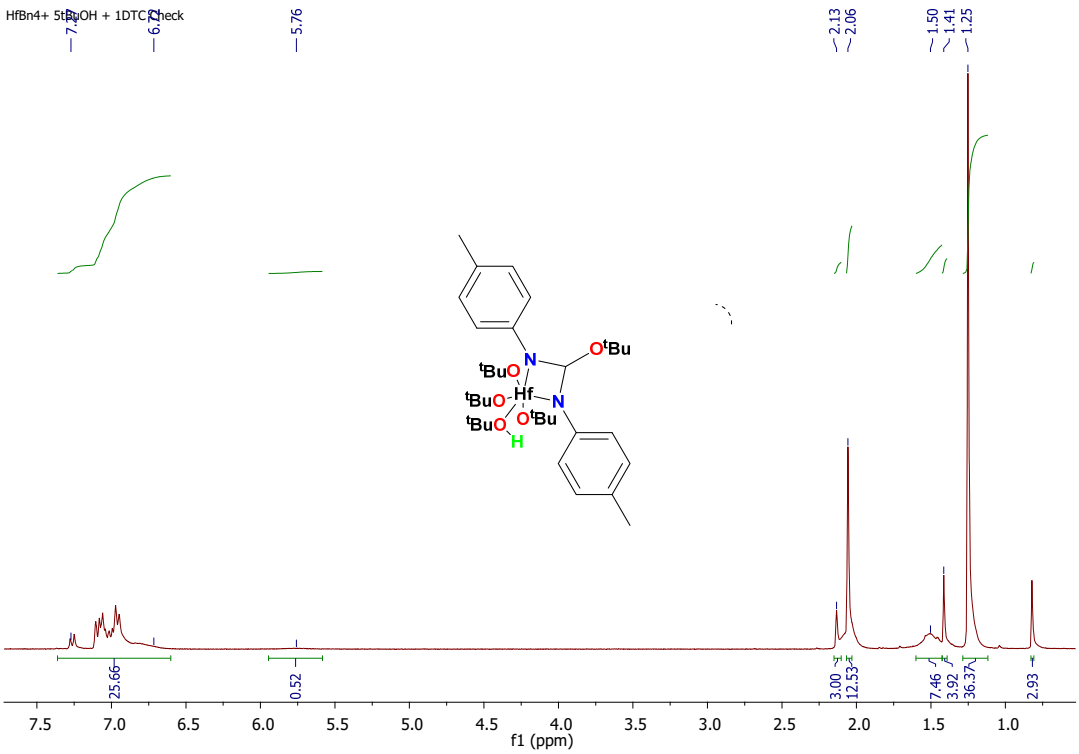

Figure S45. ^{1}H NMR of hafnium tertbutoxide reaction with DTC.

7.4. Addition of DTC to hafnium tetrabenzyl

A solution of 4equiv DTC in C_6D_6 was added to a solution of 1equiv hafnium tetrabenzyl and monitored by ^{1}HNMR. The unreacted benzylic hydrogens are at 2.7ppm and the benzylic hydrogens that form the amidinate are at 3.71ppm. in addition, the unreacted methyl group of the DTC is located at 2.00ppm and after the reaction, the group is shifted to 2.12 ppm.

^{1}H NMR (300 MHz, C_6D_6) δ 7.31(d, 2H, *H*-Ar), 7.21(d, 2H, *H*-Ar), 7.00(m, 15H, *H*-Ar), 6.87(m, 6H, *H*-Ar), 6.82(m, 4H, *H*-Ar), 6.73(d, 12H, *H*-Ar), 6.49(d, 12H, *H*-Ar), 3.71(s, 6H, *CH*$_2$-Ar), 2.70(s, 2H, *CH*$_2$-Ar), 2.12(s, 18H, *CH*$_3$), 2.00(s, 6H, *CH*$_3$).

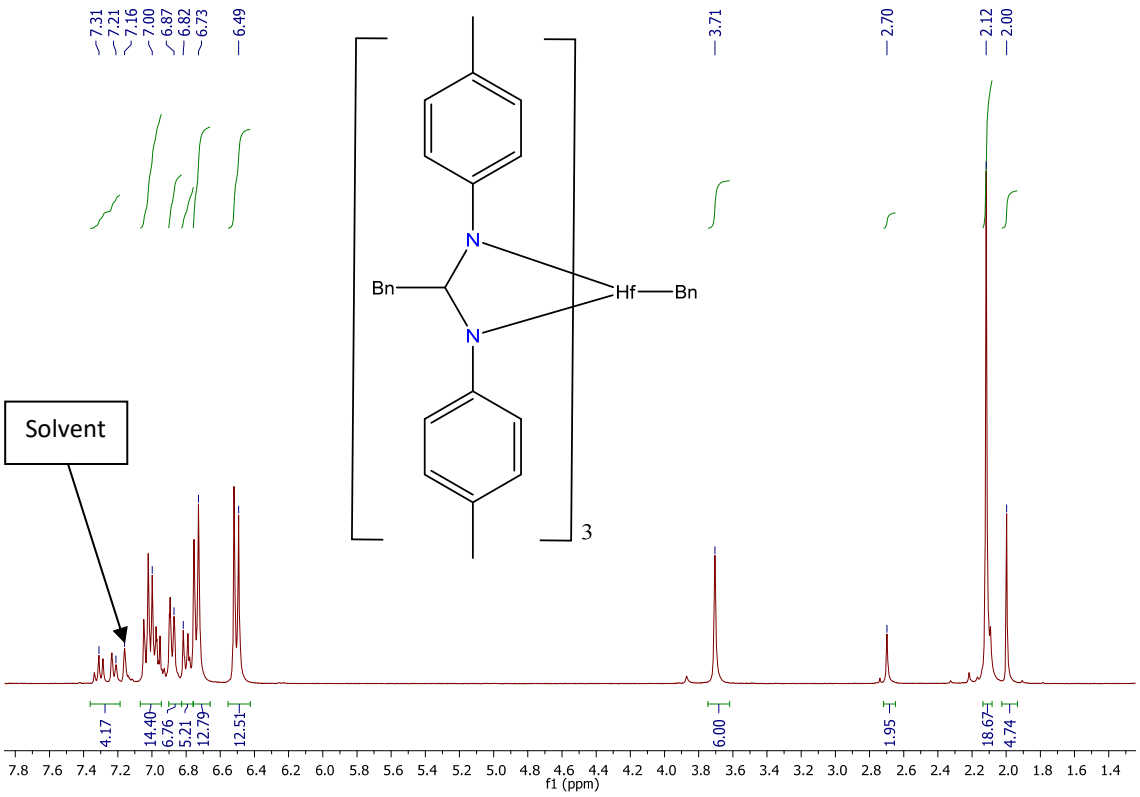

Figure S46. [1]H NMR of hafnium tetrabenzyl reaction with DTC.

7.5. Addition of 5 equiv [t]BuOH to complex **1**

A solution of 5 equiv [t]BuOH was added to a solution of 1 equiv complex **1** and monitored by [1]HNMR. The formation of 3 equiv of toluene was observed.

[1]H NMR (300 MHz, C_6D_6) δ 7.20(d, 1H, *H*-Ar), 6.95(m, 10H, *H*-Ar), 6.80(d, 5H, *H*-Ar), 6.70(d, 2H, *H*-Ar), 6.51(d, 1H, *H*-Ar), 6.16(d, 1H, *H*-Ar), 5.30(s, 1H, N-*H*), 3.72(s, 3H, C*H*$_3$), 2.64(q, 2H, C*H*(C*H*$_3$)$_2$), 2.06(s, 12H, C*H*$_3$), 1.31(s, 45H, C*H*$_3$), 1.18(d, 6H, C*H*$_3$), 0.82(d, 6H, C*H*$_3$).

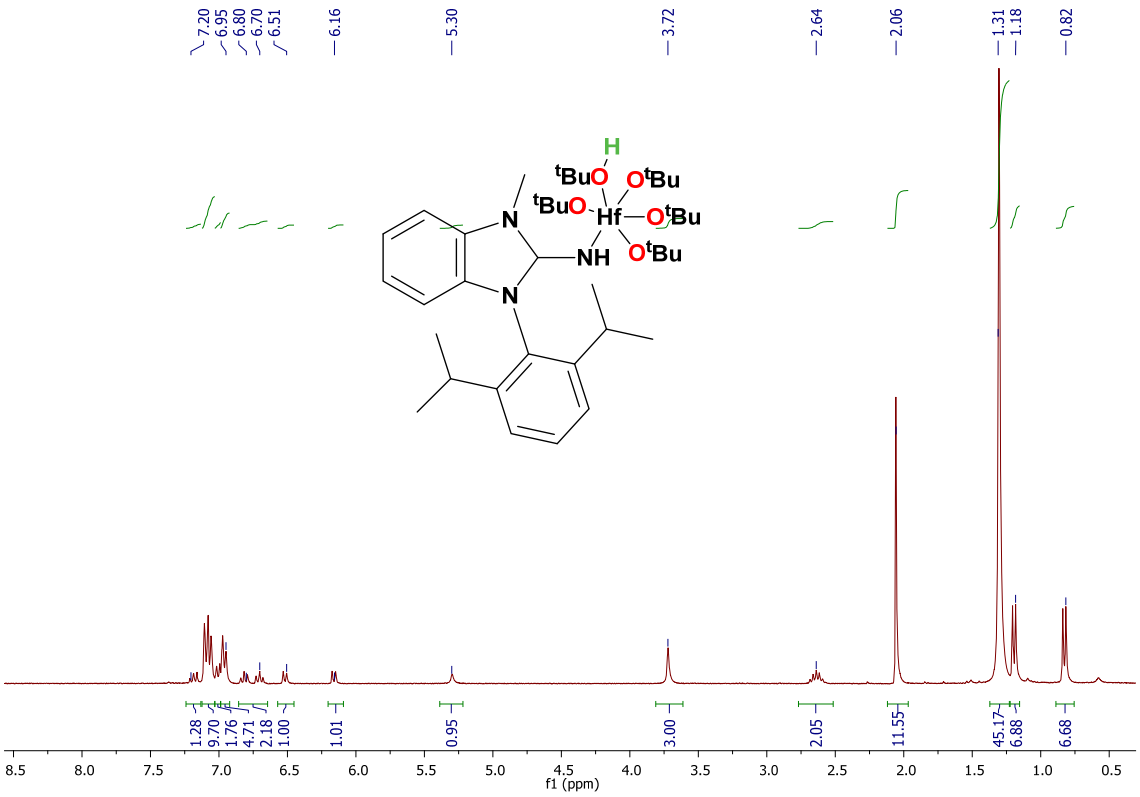

Figure S47. ^{1}H NMR of complex **1** with ^{t}BuOH.

7.6. Addition of 1 equiv DTC to complex **4** (^{t}BuOH)

A solution of hafnium tertrabenzyl and 5 equiv of tertbutyl alcohol formed *in-situ* complex **4** (^{t}BuOH), which was further reacted with 1 equiv DTC in C_6D_6. It can be seen that the ligand is neutral, indicated by the signal of the N-H at 5.24 ppm. The signal at 1.34 corresponds to the ^{t}BuO- moiety and the signal at 1.55 correspond to the product with the corresponding isourea product (N-H) at 5.76ppm.

^{1}H NMR (300 MHz, C_6D_6) δ 7.28(m, 2H, *H*-Ar), 7.10-6.95(m, 15H, *H*-Ar), 6.79-6.70(m, 4H, *H*-Ar), 6.50(d, 1H, *H*-Ar), 6.15(d, 1H, *H*-Ar), 5.76(s, 1H, N-*H*), 5.24(s, 1H, N-*H*), 3.64(s, 3H, C*H*$_3$), 2.64(q, 2H, C*H*(C*H*$_3$)$_2$), 2.12(s, 12H, C*H*$_3$), 1.55(s, 27H, C*H*$_3$), 1.34(s, 27H, C*H*$_3$), 1.16(d, 6H, C*H*$_3$), 0.84(d, 6H, C*H*$_3$).

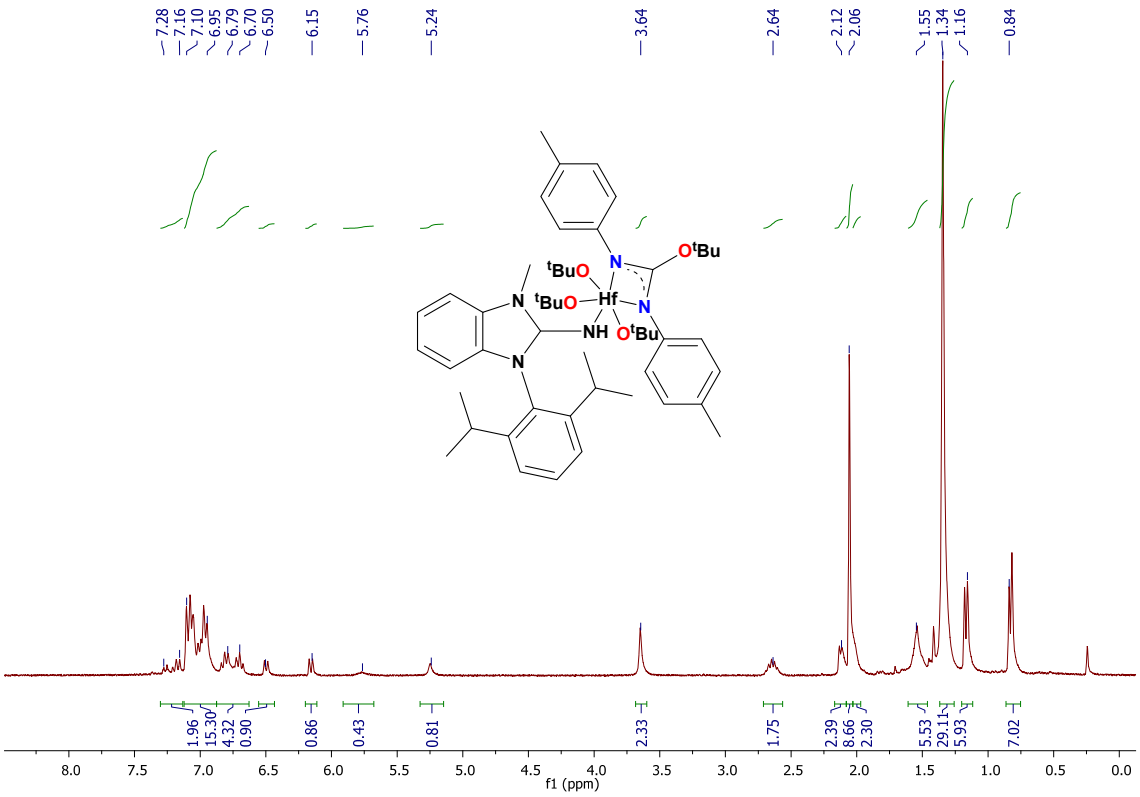

Figure S48. ^{1}H NMR of complex **4** (^{t}BuOH) with DTC.

7.7. Addition of 3 equiv DTC to complex **4** (^{t}BuOH)

A solution of hafnium tertrabenzyl and 5 equiv of tertbutyl alcohol formed the *in-situ* complex **4** and an additional 1equiv of ^{t}BuOH, which was further reacted with 3 equiv of DTC in C_6D_6. The ligand is neutral as indicated by the N-H signal at 5.19 ppm. The signal at 1.32 corresponds to the ^{t}BuO- moiety and the signal at 1.55 correspond to the product/amidinate moiety. The corresponding signal of the isourea product (N-H) is at 5.77 ppm.

^{1}H NMR (300 MHz, C_6D_6) δ 7.25(d, 2H, *H*-Ar), 7.16 (m, 1H, *H*-Ar), 7.05 (m, 8H, *H*-Ar), 6.95 (m, 20H, *H*-Ar), 6.48(d, 1H, *H*-Ar), 6.17(d, 1H, *H*-Ar), 5.19(s, 1H, N-*H*), 3.87(s, 3H, C*H*$_3$), 2.65(q, 2H, C*H*(CH$_3$)$_2$), 2.11(s, 12H, C*H*$_3$), 1.55(s, 27H, C*H*$_3$), 1.32(s, 27H, C*H*$_3$), 1.13(d, 6H, C*H*$_3$), 0.84(d, 6H, C*H*$_3$).

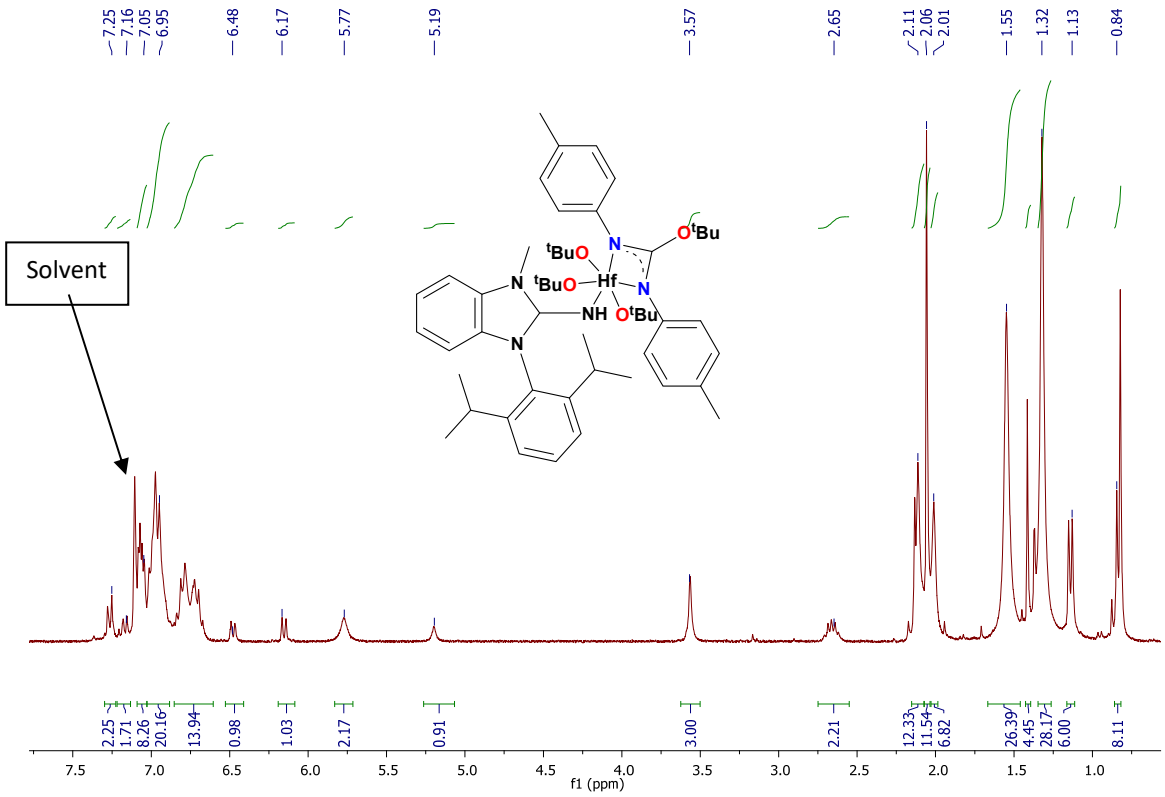

Figure S49. ^{1}H NMR of complex 4 (^{t}BuOH) with DTC.

8. IR Experiment

8.1. IR measurement of benzImidazolin-2-imine free

The following figure S50 is the IR of the free ligand, As indicated by the band at 3316 cm^{-1}. In addition, the moiety of C=N is presented at 1611 and 1632 cm^{-1}.

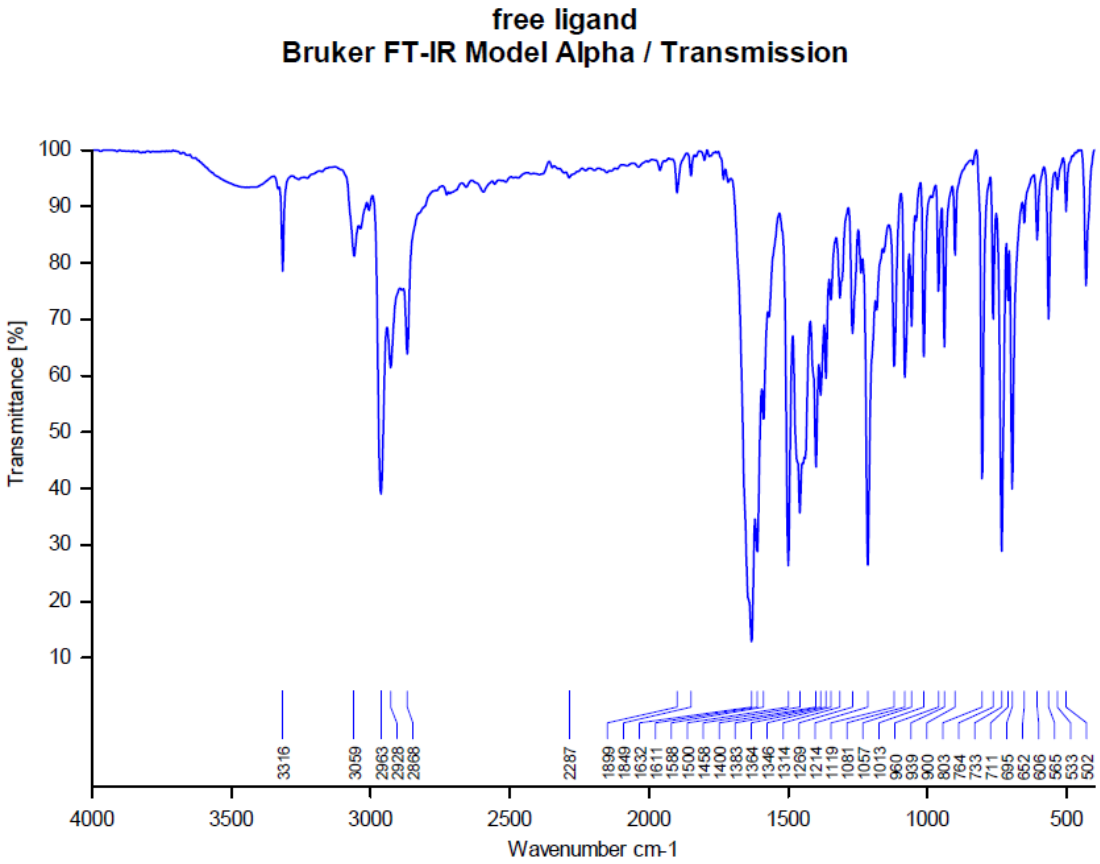

Figure S50. IR of the free ligand

8.2. IR measurement of complex **1**

Figure S51 shows the IR of complex **1**. As expected, no NH signal is observed and the bands of the C=N are at 1610 and 1635 cm^{-1}.

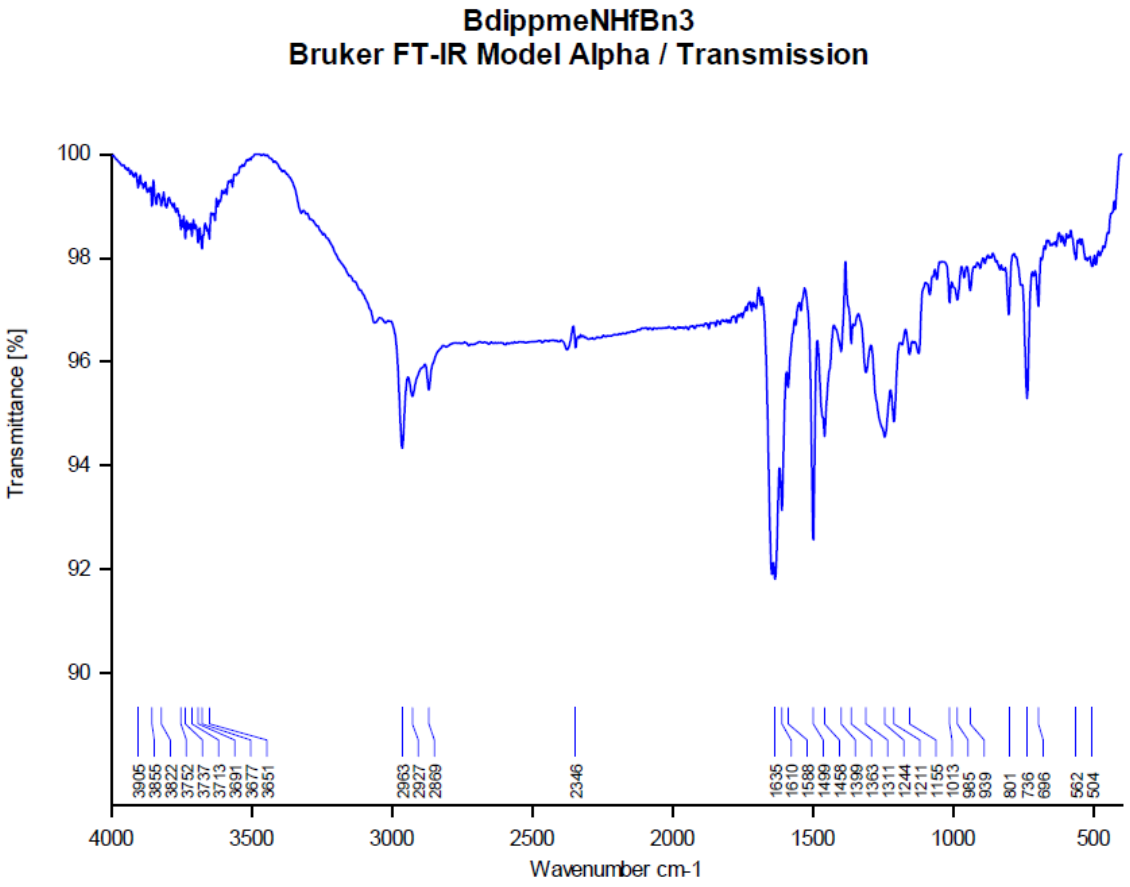

Figure S51. IR of complex **1**

8.3. IR measurement of ^{t}BuOH

The IR (figure S52) present the band of OH at 3377 cm^{-1} and the C-O bands at 1141, 1206 cm^{-1}

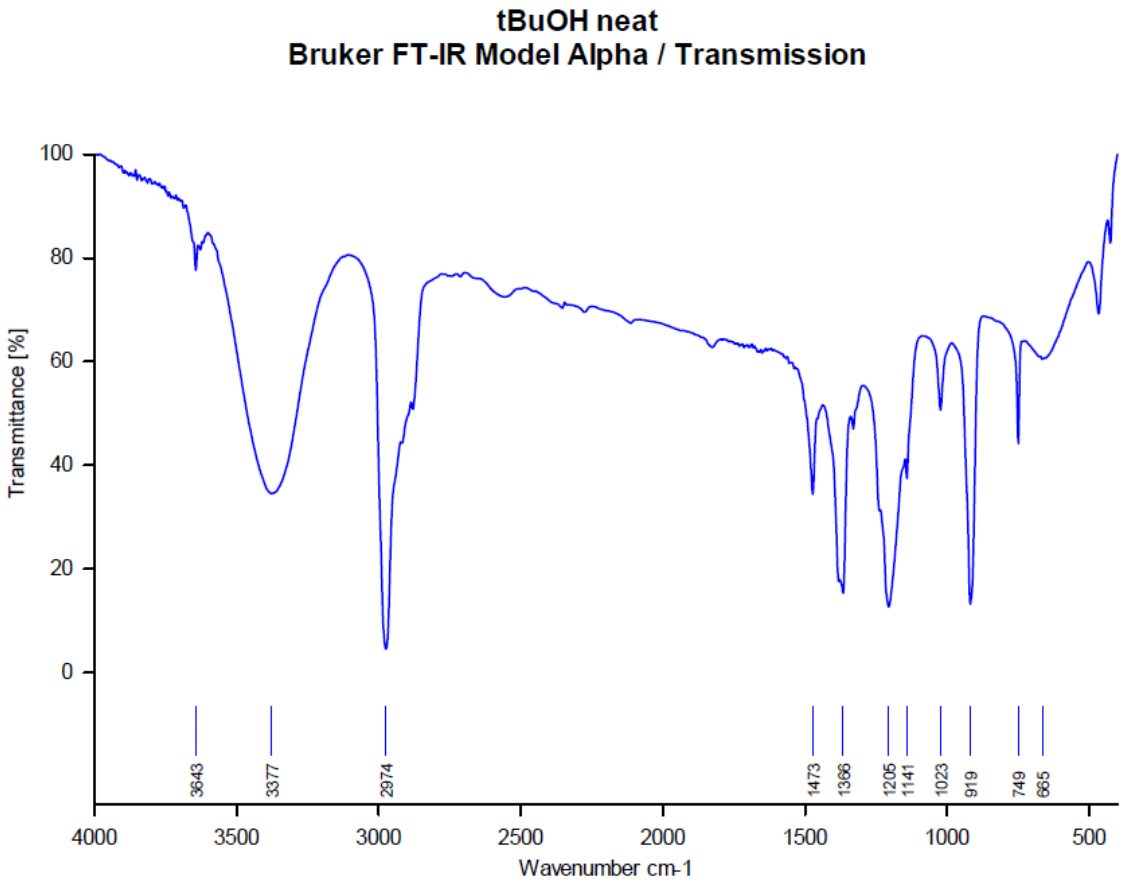

Figure S52. IR of ^{t}BuOH

8.4. IR measurement of complex **1** + ^{t}BuOH

Figure S53 shows the appearance of the N-H signal at 3328 cm^{-1}. However, there is a shift implying of a weaker N-H stretching. In addition, the signal of the O-H at 3065 cm^{-1} indicates the intermolecular O-H moiety. The C-O signals appear at 1131, 1194 cm^{-1}. And there is no free OH signal at 3377 cm^{-1}. The signal of the corresponding C=N is present at 1636 cm^{-1}.

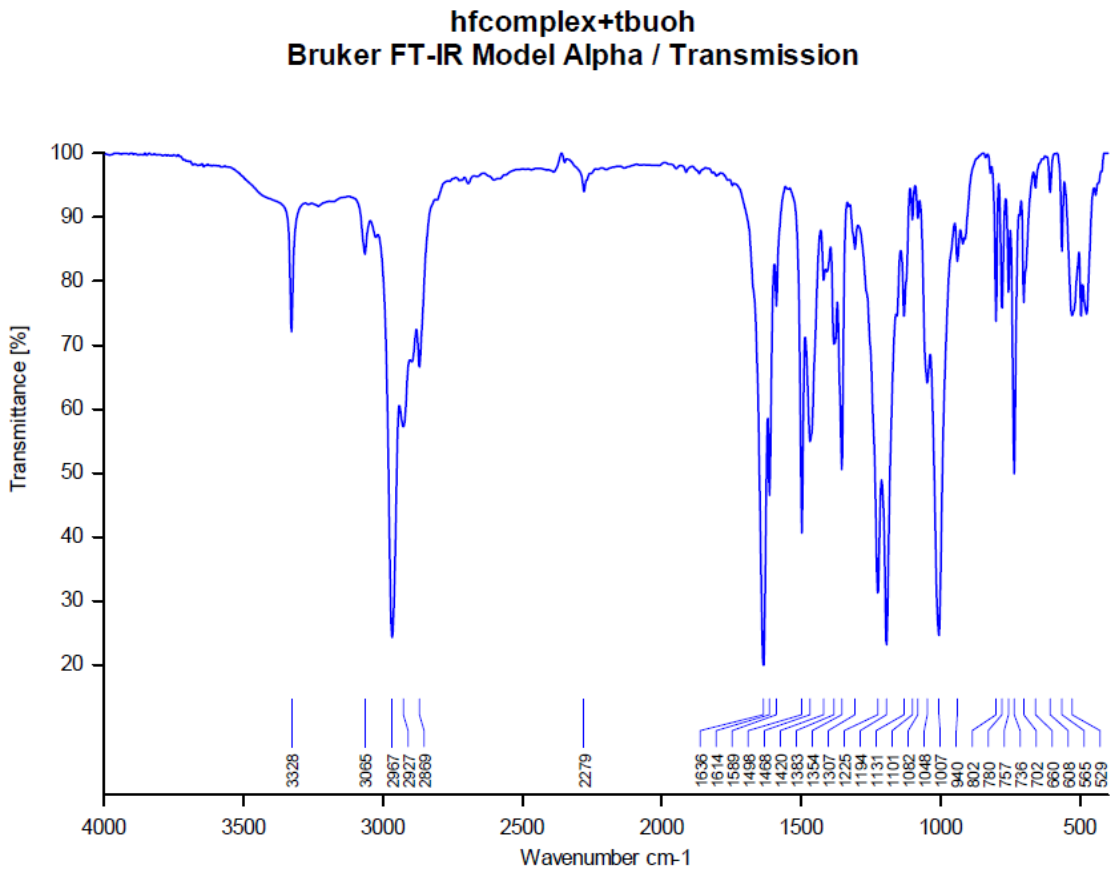

Figure S53. IR of complex **1** with 4 equiv of ^{t}BuOH

8.5. IR measurement of complex **4**

Figure S54 shows the IR of complex **4** showing the absence of the OH signal at 3377 cm^{-1} and the existence of C-O at 1200 cm^{-1} of the ^{t}BuO group.

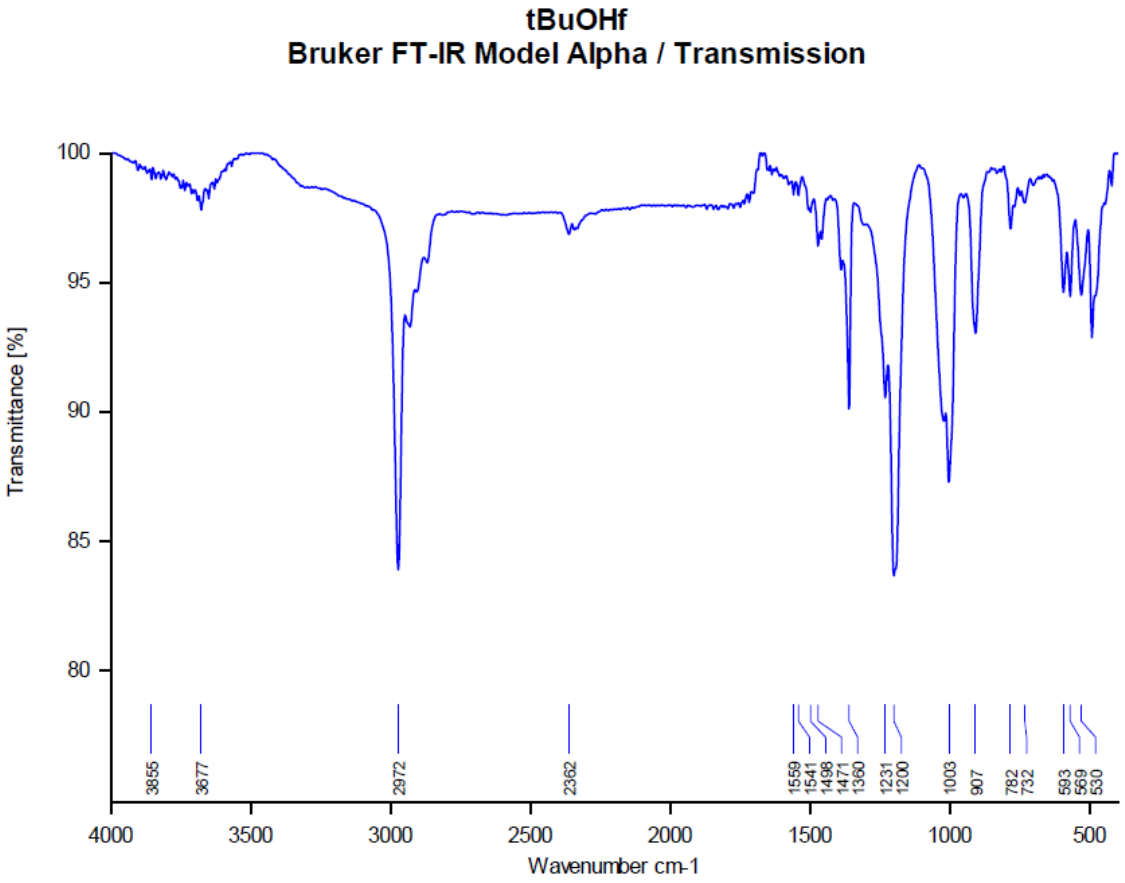

Figure S54. IR of complex **4**

8.6. IR measurement of complex **4** and the benzimidazolin-2-imine free

Figure S55 shows the IR measurement of complex **4** and benzimidazolin-2-imine free with the appearance of the N-H signal at 3326 cm^{-1} which is very close to the value indicated at S53 3328 cm^{-1} and far from the free ligand.

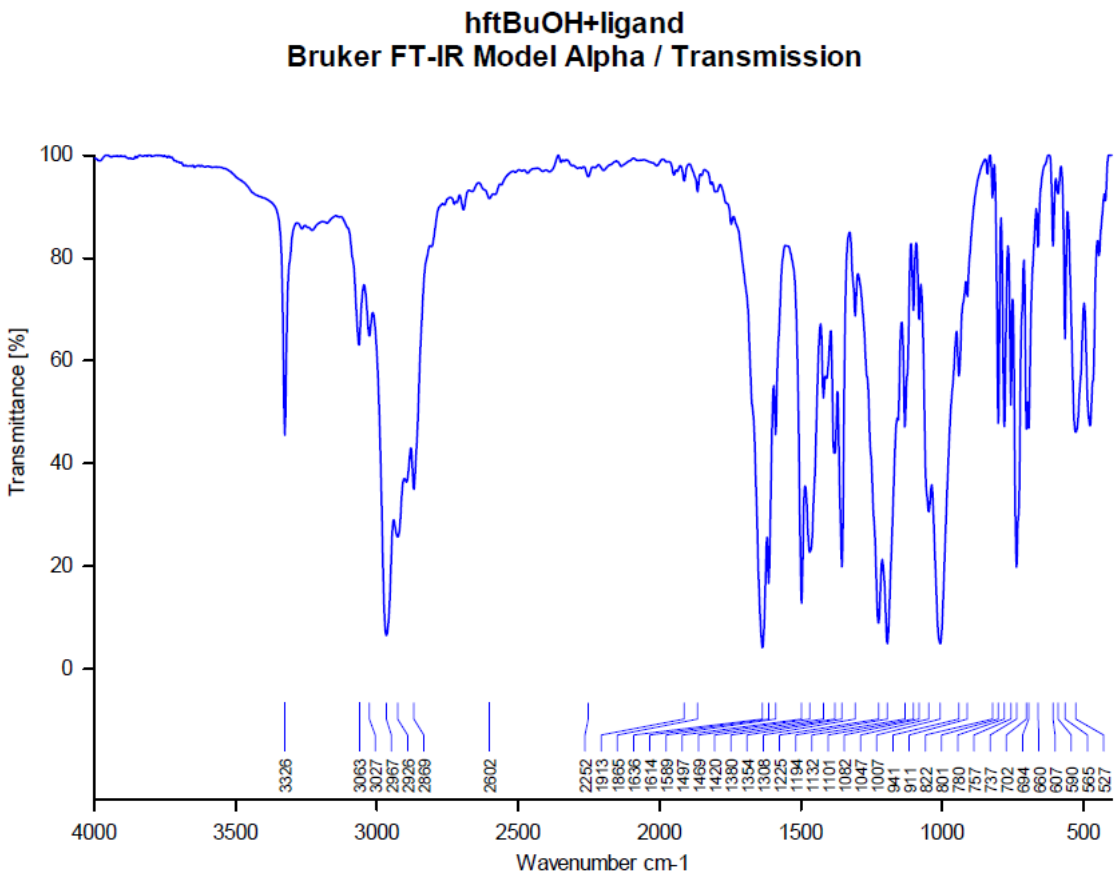

Figure S55. IR of complex **4** with the free ligand

8.7. IR measurement of ^{t}BuOD

Figure S56 shows the IR of ^{t}BuOD with the OD band at 2508 cm^{-1}.

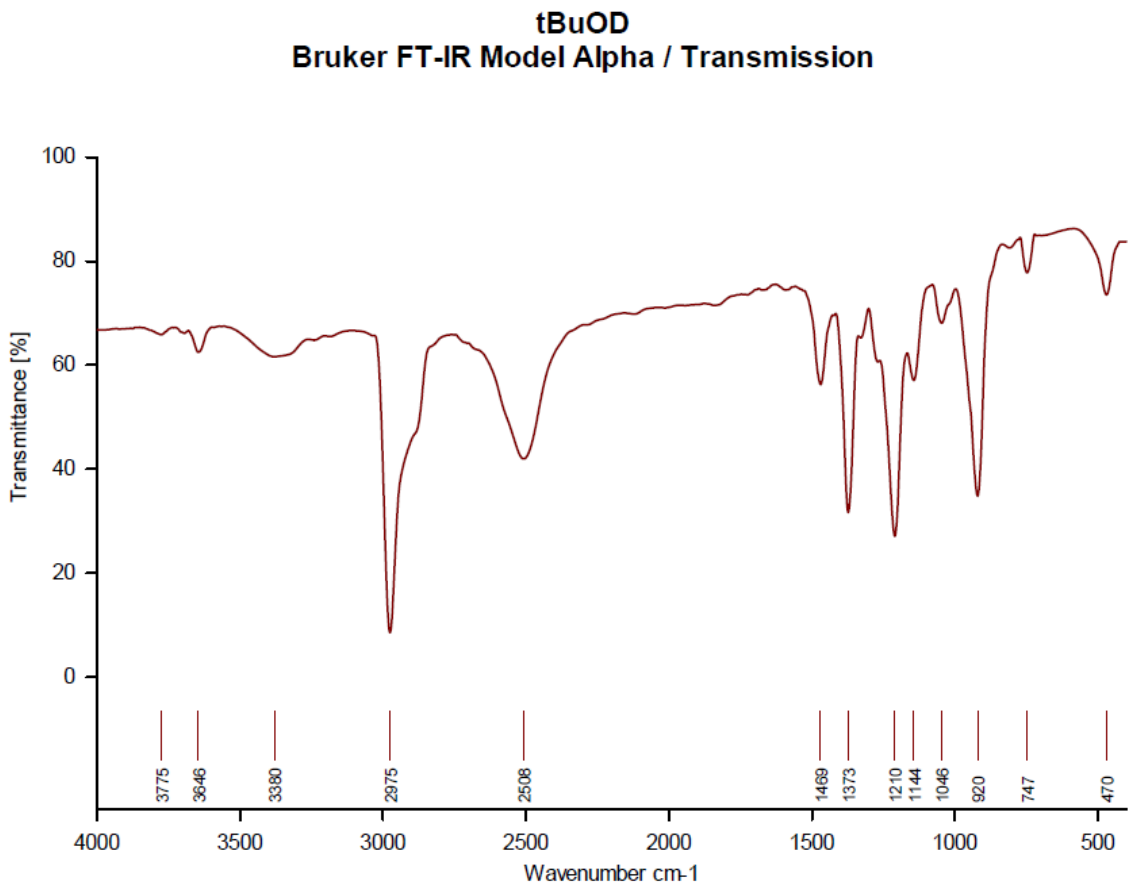

Figure S56. IR of ^{t}BuOD.

8.8. IR measurement of complex **4** + ^{t}BuOD

Figure S57 shows the IR measurement of complex **4** after the addition of ^{t}BuOD showing the ND signal at 2464 cm^{-1}.

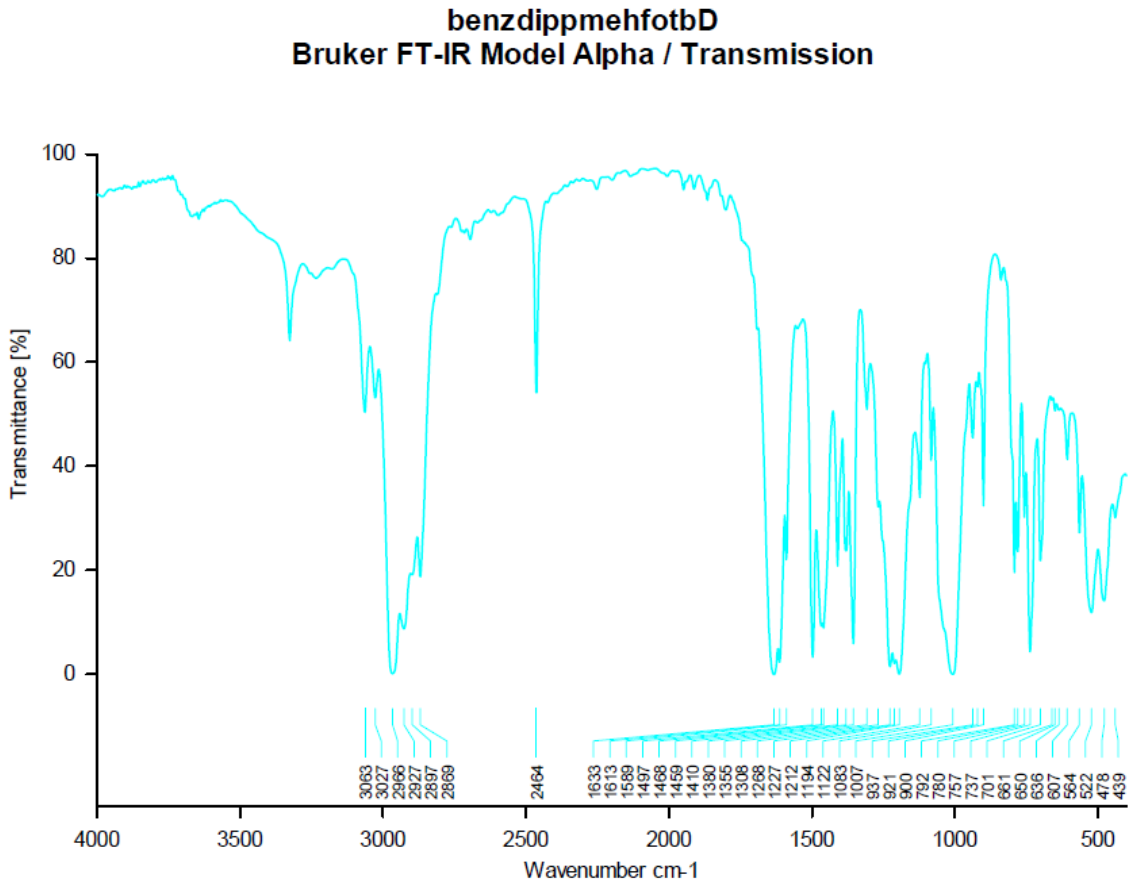

Figure S57. IR of complex **4** and ^{t}BuOD.

9. Crystallographic data

9.1. Crystallographic data of complex **1**

Empirical formula	C41 H45 Hf N3
Formula weight	758.29
Temperature	200(2) K
Wavelength	0.71073 A
Crystal system, space group	Triclinic, P -1
Unit cell dimensions	
a/Å	10.6250(10)
b/Å	12.1730(15)
c/Å	14.836(2)
α/°	109.419(6)
β/°	91.894(6)
γ/°	94.104(6)
Volume	1801.8(4) A^3
Z, Calculated density	2, 1.398 Mg/m^3
Absorption coefficient	2.926 mm^-1
F(000)	768
Crystal size	0.24 x 0.15 x 0.09 mm
Theta range for data collection	1.46 to 24.14 deg.
Limiting indices	0<=h<=11, -13<=k<=13, -16<=l<=16
Reflections collected / unique	5363 / 5363 [R(int) = 0.0470]
Completeness to theta = 24.14	99.9 %
Absorption correction	Semi-empirical from equivalents
Max. and min. transmission	0.7787 and 0.5402
Refinement method	Full-matrix least-squares on F^2
Data / restraints / parameters	5363 / 0 / 411
Goodness-of-fit on F^2	1.150
Final R indices [I>2sigma(I)]	R1 = 0.0278, wR2 = 0.0794
R indices (all data)	R1 = 0.0347, wR2 = 0.0878
Largest diff. peak and hole	1.385 and -1.043 e.A^-3

Selected Bond lengths [A] and angles [deg]:

Hf(1)-N(1)	1.917(4)
Hf(1)-C(28)	2.233(6)
Hf(1)-C(21)	2.273(5)
Hf(1)-C(35)	2.275(5)
Hf(1)-C(29)	2.805(5)
N(1)-C(1)	1.293(6)
C(1)-N(1)-Hf(1)	176.6(4)

9.2.Crystallographic data of complex **2**

Empirical formula	$C_{38}H_{39}HfN_3$
Formula weight	716.21
Temperature/K	200.15
Crystal system	triclinic
Space group	P-1
a/Å	11.469(2)
b/Å	11.763(4)
c/Å	13.145(2)
α/°	104.40(6)
β/°	94.314(10)
γ/°	101.42(5)
Volume/Å^3	1669.1(9)
Z	2
ρ_{calc}g/cm^3	1.425
μ/mm^{-1}	3.154
F(000)	720.0
Crystal size/mm^3	0.21 × 0.15 × 0.12
Radiation	MoKα (λ = 0.71073)
2Θ range for data collection/°	4.56 to 49.85
Index ranges	$0 \le h \le 13$, $-13 \le k \le 13$, $-15 \le l \le 15$
Reflections collected	5803
Independent reflections	5803 [R_{int} = 0.0810, R_{sigma} = 0.0629]
Data/restraints/parameters	5803/0/383
Goodness-of-fit on F^2	1.062
Final R indexes [I>=2σ (I)]	R_1 = 0.0455, wR_2 = 0.0663
Final R indexes [all data]	R_1 = 0.0700, wR_2 = 0.0716
Largest diff. peak/hole / e Å^{-3}	0.52/-0.56

Selected Bond lengths [A] and angles [deg]:

C(1)	N(3)	1.293(6)
C(18)	Hf(1)	2.285(6)
Hf(1)	N(3)	1.915(4)
C(32)	Hf(1)	2.259(5)
C(25)	Hf(1)	2.265(6)
C(1)	N(3) Hf(1)	174.9(4)

9.3.Crystallographic data of complex **3**

Empirical formula	$C_{34}H_{37}HfN_3$
Formula weight	666.15
Temperature/K	200.15
Crystal system	triclinic
Space group	P-1
a/Å	9.764(2)
b/Å	10.302(3)
c/Å	16.769(5)
α/°	77.291(10)
β/°	73.106(13)
γ/°	70.261(16)
Volume/Å^3	1505.2(7)
Z	2
ρ_{calc}g/cm^3	1.470
μ/mm^{-1}	3.491
F(000)	668.0
Crystal size/mm^3	0.27 × 0.24 × 0.09
Radiation	MoKα (λ = 0.71073)
2Θ range for data collection/°	4.676 to 49.872
Index ranges	$0 \le h \le 11$, $-10 \le k \le 11$, $-18 \le l \le 19$
Reflections collected	4674
Independent reflections	4674 [R_{int} = 0.0890, R_{sigma} = 0.1229]
Data/restraints/parameters	4674/0/299
Goodness-of-fit on F^2	1.047
Final R indexes [I>=2σ (I)]	R_1 = 0.0790, wR_2 = 0.1676
Final R indexes [all data]	R_1 = 0.1625, wR_2 = 0.1937
Largest diff. peak/hole / e Å^{-3}	0.74/-1.59

Selected Bond lengths [A] and angles [deg]:

Hf(1) N(1)	1.818(12)
C(1) N(1)	1.288(19)
C(14) Hf(1)	2.238(16)
C(21) Hf(1)	2.288(15)
C(28) Hf(1)	2.233(17)
C(1) N(1) Hf(1)	169.5(11)

9.4. Crystallographic data of complex **4**

Empirical formula	$C_{79}H_{120}Hf_2N_6O_8$
Formula weight	1638.78
Temperature/K	200.15
Crystal system	triclinic
Space group	P-1
a/Å	10.134(7)
b/Å	10.280(4)
c/Å	21.296(13)
α/°	82.623(10)
β/°	82.85(3)
γ/°	89.363(11)
Volume/Å^3	2183(2)
Z	1
ρ_{calc}g/cm^3	1.247
μ/mm^{-1}	2.426
F(000)	844.0
Crystal size/mm^3	0.24 × 0.18 × 0.18
Radiation	MoKα (λ = 0.71073)
2Θ range for data collection/°	3.888 to 50.002
Index ranges	$0 \le h \le 12$, $-12 \le k \le 12$, $-24 \le l \le 25$
Reflections collected	7455
Independent reflections	7455 [R_{int} = 0.0560, R_{sigma} = 0.0645]
Data/restraints/parameters	7455/0/370
Goodness-of-fit on F^2	1.094
Final R indexes [I>=2σ (I)]	R_1 = 0.0590, wR_2 = 0.1509
Final R indexes [all data]	R_1 = 0.0823, wR_2 = 0.1647
Largest diff. peak/hole / e Å^{-3}	1.56/-1.51

Selected Bond lengths [A] and angles [deg]:

Hf(1) O(1)	1.950(6)
Hf(1) O(2)	1.933(6)
Hf(1) O(3)	1.935(5)
Hf(1) O(4)	1.934(6)
Hf(1) N(1)	2.385(7)
N(1) C(1)	1.305(10)
C(1) N(1) Hf(1)	145.0(5)

9.5. Crystallographic data of complex **5**

Empirical formula	$C_{195}Hf_{14}O_{52}$
Formula weight	5672.81
Temperature/K	200.15
Crystal system	tetragonal
Space group	I-4
a/Å	34.889(6)
b/Å	34.889(6)
c/Å	10.764(2)
α/°	90
β/°	90
γ/°	90
Volume/Å^3	13102(5)
Z	2
ρ_{calc}g/cm^3	1.438
μ/mm^{-1}	5.574
F(000)	5188.0
Crystal size/mm^3	0.18 × 0.06 × 0.03
Radiation	MoKα (λ = 0.71073)
2Θ range for data collection/°	2.334 to 50.104
Index ranges	-41 ≤ h ≤ 32, -41 ≤ k ≤ 40, -11 ≤ l ≤ 12
Reflections collected	29684
Independent reflections	11376 [R_{int} = 0.1140, R_{sigma} = 0.4026]
Data/restraints/parameters	11376/55/263
Goodness-of-fit on F^2	0.813
Final R indexes [I>=2σ (I)]	R_1 = 0.0716, wR_2 = 0.1374
Final R indexes [all data]	R_1 = 0.2271, wR_2 = 0.1782
Largest diff. peak/hole / e Å^{-3}	1.82/-1.59

Selected Bond lengths [A] and angles [deg]:

Hf(1)	Hf(2)	3.215(2)
Hf(1)	O(1)	2.162(19)
Hf(1)	O(3)	2.20(2)
Hf(1)	O(4)	2.42(2)
Hf(1)	O(5)	2.03(2)
Hf(1)	O(6)	1.93(13)
Hf(1)	O(7)	1.92(2)

9.6. Crystallographic data of complex **6**

Empirical formula	$C_{114}H_{118}Hf_2N_6O_{10}$
Formula weight	2089.12
Temperature/K	296.15
Crystal system	triclinic
Space group	P-1
a/Å	13.1987(14)
b/Å	13.7686(13)
c/Å	14.1842(13)
α/°	82.556(2)
β/°	74.461(3)
γ/°	78.820(3)
Volume/Å^3	2428.1(4)
Z	1
ρ_{calc}g/cm^3	1.429
μ/mm^{-1}	2.200
F(000)	1068.0
Crystal size/mm^3	0.15 × 0.12 × 0.12
Radiation	MoKα (λ = 0.71073)
2Θ range for data collection/°	2.99 to 50.688
Index ranges	-15 ≤ h ≤ 15, -16 ≤ k ≤ 15, -14 ≤ l ≤ 16
Reflections collected	21958
Independent reflections	8563 [R_{int} = 0.1108, R_{sigma} = 0.1984]
Data/restraints/parameters	8563/0/583
Goodness-of-fit on F^2	0.809
Final R indexes [I>=2σ (I)]	R_1 = 0.0545, wR_2 = 0.1141
Final R indexes [all data]	R_1 = 0.0841, wR_2 = 0.1260
Largest diff. peak/hole / e Å^{-3}	1.85/-2.47

Selected Bond lengths [A] and angles [deg]:

Hf(1) Hf(1)^1	3.5625(7)
Hf(1) O(1)	1.962(6)
Hf(1) O(2)	2.071(5)
Hf(1) O(3)	2.007(5)
Hf(1) O(4)	2.175(5)
Hf(1) O(5)	1.942(5)

9.7. Crystallographic data of complex **7**

Identification code	Moris670b
Empirical formula	$C_{67}H_{78}HfN_3O_5$
Formula weight	1183.81
Temperature/K	296.15
Crystal system	triclinic
Space group	P-1
a/Å	11.7456(13)
b/Å	14.8900(16)
c/Å	17.998(2)
α/°	99.392(2)
β/°	97.992(3)
γ/°	98.227(4)
Volume/Å^3	3030.8(6)
Z	2
ρ_{calc}g/cm^3	1.297
μ/mm^{-1}	1.771
F(000)	1226.0
Crystal size/mm^3	0.21 × 0.18 × 0.18
Radiation	MoKα (λ = 0.71073)
2Θ range for data collection/°	2.326 to 50.454
Index ranges	$-14 \le h \le 13$, $-17 \le k \le 17$, $-21 \le l \le 21$
Reflections collected	25373
Independent reflections	10781 [R_{int} = 0.1135, R_{sigma} = 0.1629]
Data/restraints/parameters	10781/0/689
Goodness-of-fit on F^2	1.043
Final R indexes [I>=2σ (I)]	R_1 = 0.0555, wR_2 = 0.1041
Final R indexes [all data]	R_1 = 0.0842, wR_2 = 0.1178
Largest diff. peak/hole / e Å^{-3}	2.49/-1.45

Selected Bond lengths [A] and angles [deg]:

Hf-O1 = 1.989(5);
Hf-O2 = 1.922(4);
Hf-O3 = 1.983(3);
Hf-O4 = 2.072(4);
Hf-O5 = 2.002(3);

References:

(1) Tamm, M.; Petrovic, D.; Randoll, S.; Beer, S.; Bannenberg, T.; Jones, P. G.; Grunenberg, J. Structural and Theoretical Investigation of 2-Iminoimidazolines - Carbene Analogues of Iminophosphoranes. *Org. Biomol. Chem.* **2007**, 5, 523–530.

(2) Liu, H.; Khononov, M.; Fridman, N.; Tamm, M.; Eisen, M. S. Catalytic Addition of Alcohols into Carbodiimides Promoted by Organoactinide Complexes. *Inorg. Chem.* **2017**, 56, 3153–3157.

(3) Cipullo, R.; Busico, V.; Fraldi, N.; Pellecchia, R.; Talarico, G. Improving the Behavior of Bis(Phenoxyamine) Group 4 Metal Catalysts for Controlled Alkene Polymerization. *Macromolecules* **2009**, 42, 3869–3872.

(4) Kappa CCD Server Software; Nonius BV: Delft, The Netherlands, 1997.

(5) Otwinowski, Z.; Minor, W. [20] Processing of X-Ray Diffraction Data Collected in Oscillation Mode. *Methods Enzymol.* **1997**, 276, 307–326.

(6) Sheldrick, G. M. Crystal Structure Refinement with SHELXL. *Acta Crystallogr. Sect. C Struct. Chem.* **2015**, 71, 3–8.

(7) Ghatak, T.; Fridman, N.; Eisen, M. S. Actinide Complexes Possessing Six-Membered N-Heterocyclic Iminato Moieties: Synthesis and Reactivity. *Organometallics* **2017**, 36, 1296–1302.